IN THE UNITED STATES PATENT AND TRADEMARK OFFICE

In re application of: Pastan et al.
Application No. 09/763,393
Filed: July 30, 2001
Confirmation No. 5265
For: PAGE-4, AN X-LINKED GAGE-LIKE GENE EXPRESSED IN NORMAL AND NEOPLASTIC PROSTATE, TESTIS AND UTERUS, AND USES THEREFOR
Examiner: Minh-Tam Davis
Art Unit: 1642
Attorney Reference No. 4239-61541-01

CERTIFICATE OF MAILING

I hereby certify that this paper and the documents referred to as being attached or enclosed herewith are being deposited with the United States Postal Service as First Class Mail in an envelope addressed to: MAIL STOP AMENDMENT COMMISSIONER FOR PATENTS, P.O. BOX 1450, ALEXANDRIA, VA 22313-1450 on the date shown below.

Attorney or Agent for Applicant(s)

Date Mailed March 13, 2006

MAIL STOP AMENDMENT
COMMISSIONER FOR PATENTS
P.O. BOX 1450
ALEXANDRIA, VA 22313-1450

DECLARATION OF DR. PASTAN UNDER 37 CFR § 1.132

1. I, Ira Pastan, M.D., am an inventor of the above-referenced application.

2. It is my understanding that claims 1-8, 14-15, 17-18, 53, 55, 57 were rejected in the Office action dated August 5, 2004, as allegedly not being enabled by the specification. In addition, claims 1-8, 14-15, 17-18 53, 55 and 57 were rejected as allegedly there is insufficient written description for one of skill in the art to make and use the claimed invention, as polypeptides with "unknown structure" are included. In addition, claims 1-8, 14-15, 17-18, 53, 55 and 57 are rejected as not having any utility, as allegedly one of skill in the art would not know that PAGE4 polypeptides, and immunogenic fragments thereof, could be used to treat cancer based on the specification.

3. The specification includes sufficient written description of PAGE4 (shown in SEQ ID NO: 1), and immunogenic epitopes of PAGE4. The amino acid sequence of PAGE4 is provided as SEQ ID NO: 1 of the specification. This amino acid sequence is 102 amino acids in length.

Immunogenic peptides are clearly described in the specification. For example, immunogenic peptides, such as peptides that bind MHC are disclosed in the specification on page 7, line 35 to page 8, line 25, and on page 20, line 1 to page 22, line 5. The specification also discloses that epitopes of use are 8-10 amino acids in length and have anchoring residues. Specific configurations of use are disclosed, such as wherein the PAGE4 polypeptides is 9 or 10 amino acids in length and includes binding motifs for HLA-A2 (see, for example, page 8, lines 30-37, page 20, to page 21, line 2, and page 21, lines 15-19), such as those peptides that have specific anchoring residues in the second position and a positively charged amino acid at the position nine (see page 20, line 20 to page 21, line 2). The selection of binding motifs that bind HLA-A2 is further described on page 28, line 25 to page 29, line 29). Methods and computer based programs for predicting MHC binding motifs (immunogenic epitopes) were disclosed in the specification (for example, see page 8, lines 12-25 and page 21, line 34 to page 22, line 5), were well known to those of skill in the art at the time the provisional application was filed (see for example, Parker et al., Scheme for ranking potential HLA-A2 binding peptides based on independent binding of individual peptide side-chains. J Immunol 152:163-75, 1994). In addition, biological methods of testing whether a specific epitope is immunogenic are also provided (for example, see page 8, lines 1-4 and page 21, lines 3-12 and lines 20-29).

4. Using the information disclosed in the specification, the primary amino acid sequence of human PAGE4 was analyzed for consensus motifs for novel HLA-A2 binding peptides using a computer program. Specifically, the amino acid sequence of PAGE4 was scanned for matches to consensus motifs for HLA-A2 binding peptides. My colleagues and I used the computer algorithm from the BioInformatics and Molecule Analysis Section of NIH (BIMAS) (developed by Parker et al. (see the article published in J Immunol 152:163-75, 1994 for a complete description), which ranks potential MHC binding peptides according to the predictive one-half-time dissociation of peptide/MHC complexes. The HLA-A2 allele was chosen because it is the most commonly expressed class I allele. Nine-mer and ten-mer peptides were synthesized if they conformed to the respective consensus motif; binding of immunogenic peptides to this allele is disclosed in the specification, such as on page 20, lines 10-19. A panel of PAGE4 peptides (Table 1) were made by Biosynthesis Inc. (Lewisville, Texas) with a purity >95%. A MUC-1 peptide and a carcinoembryonic antigen (CEA) HLA-A3 binding peptide (CAP-7) were used as

a positive and negative control, respectively (Tsang et al, J Natl Cancer Inst 87:982-90, 1995). Binding of PAGE4 peptides and the PAGE4 analogues to HLA-A2 molecules was evaluated by the upregulation of HLA-A2 expression on T2 cells as demonstrated by flow cytometry (Njiman et al., Eur J Immunol 23:1215-9, 1993). As shown in Table 1, two of three native peptides (P16, P84) bound to HLA-A2 molecules in the T2 assay.

Table 1. Binding of PAGE4 peptides to HLA-A2 molecules

Peptides	Designation	Amino acid position	Peptide sequence	T2 binding[a]
P16 (native)	test	16-25	QEAPDVVAFV	309 (1.2)
P59 (native)	test	59-68	VEGDCQEMDL	246 (0.9)
P84 (native)	test	84-92	KTPPNPKHA	270 (1.04)
CAP-7 peptide	(negative control)		HLFGYSWYK	260

Studies were then undertaken to examine the stability of the peptide-MHC complex for the peptides P16 and P84. Each peptide was incubated with T2 cells overnight, the unbound peptides were washed off, and the cells were then incubated with Brefeldin A to block delivery of new class I molecules to the cell surface. Cells were analyzed for the presence of peptide-HLA-A2 complexes at various time points. For both peptides, more than 43.6% of complexes remained over the 8-hour observation period.

5. Studies were conducted to determine whether T-cell lines could be generated from peripheral blood mononuclear cells (PBMC) from prostate cancer patients. Autologous dendritic cells (DCs) were used as antigen presenting cells (APC). PAGE4-specific T-cell lines were generated from a prostate cancer patient (termed patient "A") using P16 and P84. Specifically, modification of the protocol described by Tsang et al. (J Natl Cancer Inst 87:982-90, 1995) was used to generate PAGE4-specific CTLs. Irradiated (3000 rad) autologous DCs were used as APCs.

Autologous non-adherent cells were stimulated in the presence of autologous DCs pulsed with peptides at a concentration of 12.5 μg/ml at an effector-to-APC ratio of 10:1. Cultures were maintained for three initial days in medium containing 10% human AB serum, and four

additional days in the same medium supplemented with 20 units/ml of recombinant human IL-2. After a 7-day culture period, designated as an *in vitro* stimulation (IVS) cycle, cells were restimulated as described above for a total of three IVS. After the third IVS cycle, irradiated (23,000 rads) autologous Epstein-Barr virus (EBV) - transformed B cells were used as APCs. The autologous EBV-transformed B cells were pulsed with 12.5 μg/ml of peptides at an effector-to-APC ratio of 1:3.

The T-cell lines were designated T-A-P16 or T-A-P84. The specificity of the PAGE4-specific T cells was analyzed for their ability to release IFN-γ after stimulation with autologous B cells pulsed with the corresponding peptides. Specifically, supernatants of T cells stimulated for 48 hours with peptide-pulsed autologous EBV-transformed B cells, in IL-2-free medium at various peptide concentrations, were screened for secretion of IFN-γ using an ELISA kit (BioSource International, Camarillo, CA) and lymphotactin using an ELISA assay (Muller et al., Eur J Immunol 25: 1744-8, 1995).

As shown in Table 2, high levels of IFN-γ production were observed when the T-cell lines were stimulated with the specific peptide, although higher levels of IFN-γ production was observed for the T-A-P16 T-cell line for the T-A-P84 T-cell line.

Table 2. Production of IFN-γ by T-cell lines generated from a prostate cancer patient stimulated with P16 or P84

	Production of IFN-γ (pg/ml)	
T-cell line	Corresponding peptide	None
T-A-P16	302.0	<15.6
T-A-P84	97.5	<15.6

6. To examine the ability of the P16 peptide to activate the PAGE4-specific T-cells, T-A-P16 cells were analyzed to determine their ability to lyse peptide-pulsed targets. Specifically, a 6-hour or 16-hour ^{111}In release assay was used to determine T-cell mediated killing (Tsang et al., J Natl Cancer Inst 87:982-90, 1995. Target cells were labeled with ^{111}In oxine (Amersham Health, Silver Spring, MD) for 20 minutes at room temperature. For these assays, 3 X 10^3 cells were used per well, in 96-well rounded-bottom culture plates. ^{111}In release was measured by

gamma counting. Spontaneous release was determined by incubating the target cells with medium alone, and complete lysis by incubating the target cells with 2.5% Triton X-100. Specific lysis (%) = [(observed release – spontaneous release)/(complete release – spontaneous release)] X 100.

The results were expressed as percent specific lysis at effector-to-target ratio of 30:1 and 15:1. Labeled T2 cells were incubated with or without peptide (12.5 μg/ml) in serum-free medium for 2 hours at 37°C prior to their addition into the assay. Effector cells were used at IVS4. As shown in Table 3, lysis of T2 cells pulsed with the P16 peptide lysed target cells, at two different E:T cell ratios.

Table 3. Ability of the PAGE4-specific T-cell lines (T-A-P16) to lyse peptide-pulsed targets

Target	% lysis (±SD)*			
	T-A-P16		T-B-P16-1	
	30 : 1	15 : 1	30 : 1	15 : 1
T2	5.1 (1.1)	6.4 (0.2)	7.6 (0.1)	6.6 (0.9)
T2 + P16	12.7 (1.7)	9.1 (0.9)	23.5 (0.6)	22.7 (0.8)

CTL degranulation is a requisite process of perforin-granzyme mediated killing by activated CD8+ T cells. Thus, to confirm that the CD8+ cells were indeed activated, CD107a mobilization to the cell surface of CD8+ T cells was examined following activation with P16 peptide in addition to CTL assays. The CD107a mobilization assay was performed according to a method known in the art (see Rubio et al., Nat Med 9:1377-82, 2003). CD8+ T cells stimulated with P16 expressed surface CD107a.

7. Studies were then conducted to determine whether the PAGE4-specific T-cell lines could lyse tumor cells that endogenously express native PAGE4. The expression of HLA-A2 and PAGE4 on tumor cell lines was analyzed by flow cytometry and RT-PCR, respectively. It was demonstrated that T-A-P16 cells were capable of lysing LNCaP human prostate cancer cells that express native PAGE4 and are HLA-A2 positive. At an effector: target ratio of 30:1 approximately 15% of the target cells were lysed, while at an effector:target ratio of 15:1 approximately 8% of the target cells were lysed.

8. These studies demonstrate that immunogenic fragments of PAGE4 can be produced and used to activate lymphocytes, as described in the specification. In addition, the results demonstrate that immunogenic PAGE4 fragments can be used to induce an immune response that results in the lysis of prostate cancer cells. The results presented above (points 2-7) support that one of skill in the art, such as myself, could readily use the disclosure of the above-referenced application to produce peptide fragments of SEQ ID NO: 1 and test their immunogenicity. I and my colleagues have produced variant peptide sequences (with an altered amino acid sequence) that have a high binding affinity for MHC, and can be used to activate T cells. These variant polypeptides are disclosed in a U.S. Provisional Application filed on February 24, 2005 (inventors are Jeffrey Schlom, Kwong-Yok Tsang, and Ira Pastan).

9. It is my understanding that claims 1-8, 14-15, 17-18, 53, 55, 57 were rejected in the Office action dated August 5, 2004, as allegedly one of skill in the art could not determine that SEQ ID NO: 1 or a fragment thereof would have a credible utility. The Office action asserts that one of skill in the art could not predict, based on an mRNA analysis, that encoded protein would be differentially expressed in prostate and uterine cancer. It is my understanding that the Office action asserts (page 14) that protein levels cannot be predictably correlated with either steady state mRNA levels or alterations in mRNA levels for any cancer, thus there cannot be a utility for PAGE4 protein. I disagree with this assertion.

PAGE4 expression is highly expressed in prostate and uterine cancer. Ornstoft et al. (Molec. Cell Proteomics 1: 37-45, 2002, copy submitted herewith as Exhibit A) has performed a genome-wide study of gene copy numbers, transcripts and protein levels in pairs of non-invasive and invasive human carcinomas. Although it was only possible to compare mRNA and protein in a few cases (due to a limited ability to focus some of the proteins on two dimensional gels), there was a good correlation ($p<0.005$) between transcript alterations and protein levels. Based on this study, one of skill in the art would predict that the presence (or absence) of PAGE4 mRNA would correlate with the presence (or absence of PAGE4 protein).

Northern blot and reverse transcriptase polymerase chain reaction (see page 4, line 30 to page 5, line 6; page 5, lines 16-20; and FIGS. 3 and 5) were used to evaluate the expression of PAGE4 in cancer. Polyclonal antibodies (see Example 3, page 41 of the specification) were used

to determine if PAGE4 protein was expressed in prostate cancer. Western blot analysis confirmed that PAGE4 was expressed in a prostate cancer lysate (see Fig. 2B of Iavrone et al., Mol. Cancer Therap. 1: 329-335, 2002, copy submitted herewith as Exhibit B). We analyzed samples of prostate cancer from five patients whose cancers expressed PAGE4 mRNA. PAGE4 protein was expressed in all five of these samples (a 100% correlation). To determine the localization of PAGE4 in the cell, nuclear cytoplasmic and membrane fractions (see Wolfgang et al., PNAS 97: 9437-9443, 2000) were prepared from NIH3T3 cells and prostate cancer cells (PC3) stably expressing PAGE4 mRNA. The PAGE4 protein product was detected in the cytoplasmic fraction of these cell lines. Immunohistochemical analyses were performed on NIH3T3 cells transfected with an expression vector encoding PAGE 4. These immunohistochemical studies confirmed that the PAGE4 protein can be detected in the cytoplasm (see FIG. 4 of Iavrone et al., *supra*). The correlation of PAGE4 mRNA with the presence of PAGE4 protein in prostate cancer, and the showing that PAGE4 protein can be detected in cells expressing PAGE4 mRNA documents the utility of the PAGE4 protein.

10. I hereby declare that all statements made herein of my own knowledge are true and that all statements made on information and belief are believed to be true; and further that these statements were made with the knowledge that willful false statements and the like so made are punishable by fine or imprisonment, or both, under Section 1001 of the Title 18 of the United States Code, and that such willful false statements may jeopardize the validity of the application or any patent issued thereon.

Ira Pastan, M.D.

3/10/06
Date

Genome-wide Study of Gene Copy Numbers, Transcripts, and Protein Levels in Pairs of Non-invasive and Invasive Human Transitional Cell Carcinomas*

Torben F. Ørntoft‡§, Thomas Thykjaer¶, Frederic M. Waldman‖, Hans Wolf**, and Julio E. Celis‡‡

Gain and loss of chromosomal material is characteristic of bladder cancer, as well as malignant transformation in general. The consequences of these changes at both the transcription and translation levels is at present unknown partly because of technical limitations. Here we have attempted to address this question in pairs of non-invasive and invasive human bladder tumors using a combination of technology that included comparative genomic hybridization, high density oligonucleotide array-based monitoring of transcript levels (5600 genes), and high resolution two-dimensional gel electrophoresis. The results showed that there is a gene dosage effect that in some cases superimposes on other regulatory mechanisms. This effect depended ($p < 0.015$) on the magnitude of the comparative genomic hybridization change. In general (18 of 23 cases), chromosomal areas with more than 2-fold gain of DNA showed a corresponding increase in mRNA transcripts. Areas with loss of DNA, on the other hand, showed either reduced or unaltered transcript levels. Because most proteins resolved by two-dimensional gels are unknown it was only possible to compare mRNA and protein alterations in relatively few cases of well focused abundant proteins. With few exceptions we found a good correlation ($p < 0.005$) between transcript alterations and protein levels. The implications, as well as limitations, of the approach are discussed. ***Molecular & Cellular Proteomics 1:37–45, 2002.***

Aneuploidy is a common feature of most human cancers (1), but little is known about the genome-wide effect of this phenomenon at both the transcription and translation levels. High throughput array studies of the breast cancer cell line BT474 has suggested that there is a correlation between DNA copy numbers and gene expression in highly amplified areas (2), and studies of individual genes in solid tumors have revealed a good correlation between gene dose and mRNA or protein levels in the case of c-erb-B2, *cyclin d1*, *ems1*, and N-myc (3–5). However, a high cyclin D1 protein expression has been observed without simultaneous amplification (4), and a low level of c-myc copy number increase was observed without concomitant c-myc protein overexpression (6).

In human bladder tumors, karyotyping, fluorescent *in situ* hybridization, and comparative genomic hybridization (CGH)[1] have revealed chromosomal aberrations that seem to be characteristic of certain stages of disease progression. In the case of non-invasive pTa transitional cell carcinomas (TCCs), this includes loss of chromosome 9 or parts of it, as well as loss of Y in males. In minimally invasive pT1 TCCs, the following alterations have been reported: 2q−, 11p−, 1q+, 11q13+, 17q+, and 20q+ (7–12). It has been suggested that these regions harbor tumor suppressor genes and oncogenes; however, the large chromosomal areas involved often contain many genes, making meaningful predictions of the functional consequences of losses and gains very difficult.

In this investigation we have combined genome-wide technology for detecting genomic gains and losses (CGH) with gene expression profiling techniques (microarrays and proteomics) to determine the effect of gene copy number on transcript and protein levels in pairs of non-invasive and invasive human bladder TCCs.

EXPERIMENTAL PROCEDURES

Material—Bladder tumor biopsies were sampled after informed consent was obtained and after removal of tissue for routine pathology examination. By light microscopy tumors 335 and 532 were staged by an experienced pathologist as pTa (superficial papillary),

From the ‡Department of Clinical Biochemistry, Molecular Diagnostic Laboratory and **Department of Urology, Aarhus University Hospital, Skejby, DK-8200 Aarhus N, Denmark, ¶AROS Applied Biotechnology ApS, Gustav Wiedsvej 10, DK-8000 Aarhus C, Denmark, ‖UCSF Cancer Center and Department of Laboratory Medicine, University of California, San Francisco, CA 94143-0808, and ‡‡Institute of Medical Biochemistry and Danish Centre for Human Genome Research, Ole Worms Allé 170, Aarhus University, DK-8000 Aarhus C, Denmark

Received, September 26, 2001, and in revised form, November 7, 2001

Published, MCP Papers in Press, November 13, 2001, DOI 10.1074/mcp.M100019-MCP200

[1] The abbreviations used are: CGH, comparative genomic hybridization; TCC, transitional cell carcinoma; LOH, loss of heterozygosity; PA-FABP, psoriasis-associated fatty acid-binding protein; 2D, two-dimensional.

EXHIBIT A

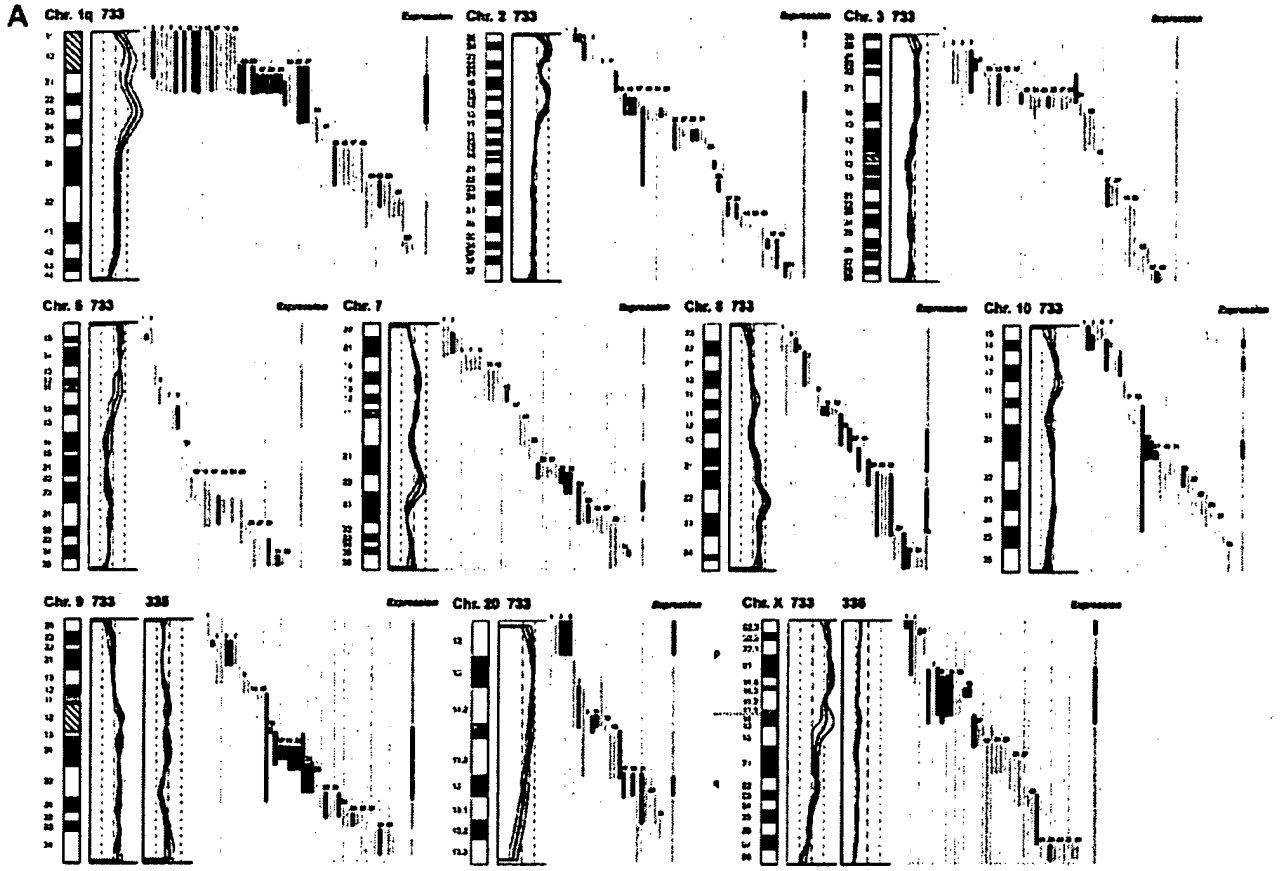

FIG. 1. **DNA copy number and mRNA expression level.** Shown from *left* to *right* are chromosome (*Chr.*), CGH profiles, gene location and expression level of specific genes, and overall expression level along the chromosome. *A*, expression of mRNA in invasive tumor 733 as compared with the non-invasive counterpart tumor 335. *B*, expression of mRNA in invasive tumor 827 compared with the non-invasive counterpart tumor 532. The average fluorescent signal ratio between tumor DNA and normal DNA is shown along the length of the chromosome (*left*). The *bold curve* in the ratio profile represents a mean of four chromosomes and is surrounded by *thin curves* indicating one standard deviation. The *central vertical line* (*broken*) indicates a ratio value of 1 (no change), and the *vertical lines* next to it (*dotted*) indicate a ratio of 0.5 (*left*) and 2.0 (*right*). In chromosomes where the non-invasive tumor 335 used for comparison showed alterations in DNA content, the ratio profile of that chromosome is shown to the *right* of the invasive tumor profile. The *colored bars* represents one gene each, identified by the running *numbers above* the *bars* (the name of the gene can be seen at www.MDL.DK/sdata.html). The *bars* indicate the purported location of the gene, and the *colors* indicate the expression level of the gene in the invasive tumor compared with the non-invasive counterpart; >2-fold increase (*black*), >2-fold decrease (*blue*), no significant change (*orange*). The *bar* to the *far right*, entitled *Expression* shows the resulting change in expression along the chromosome; the *colors* indicate that at least half of the genes were up-regulated (*black*), at least half of the genes down-regulated (*blue*), or more than half of the genes are unchanged (*orange*). If a gene was absent in one of the samples and present in another, it was regarded as more than a 2-fold change. A 2-fold level was chosen as this corresponded to one standard deviation in a double determination of ~1800 genes. Centromeres and heterochromatic regions were excluded from data analysis.

grade I and II, respectively, tumors 733 and 827 were staged as pT1 (invasive into submucosa), 733 was staged as solid, and 827 was staged as papillary, both grade III.

mRNA Preparation—Tissue biopsies, obtained fresh from surgery, were embedded immediately in a sodium-guanidinium thiocyanate solution and stored at −80 °C. Total RNA was isolated using the RNAzol B RNA isolation method (WAK-Chemie Medical GMBH). poly(A)$^+$ RNA was isolated by an oligo(dT) selection step (Oligotex mRNA kit; Qiagen).

cRNA Preparation—1 μg of mRNA was used as starting material. The first and second strand cDNA synthesis was performed using the SuperScript® choice system (Invitrogen) according to the manufacturer's instructions but using an oligo(dT) primer containing a T7 RNA polymerase binding site. Labeled cRNA was prepared using the MEGAscrip® *in vitro* transcription kit (Ambion). Biotin-labeled CTP and UTP (Enzo) was used, together with unlabeled NTPs in the reaction. Following the *In vitro* transcription reaction, the unincorporated nucleotides were removed using RNeasy columns (Qiagen).

Array Hybridization and Scanning—Array hybridization and scanning was modified from a previous method (13). 10 μg of cRNA was fragmented at 94 °C for 35 min in buffer containing 40 mM Tris acetate, pH 8.1, 100 mM KOAc, 30 mM MgOAc. Prior to hybridization, the fragmented cRNA in a 6× SSPE-T hybridization buffer (1 M NaCl, 10 mM Tris, pH 7.6, 0.005% Triton), was heated to 95 °C for 5 min, subsequently cooled to 40 °C, and loaded onto the Affymetrix probe array cartridge. The probe array was then incubated for 16 h at 40 °C at constant rotation (60 rpm). The probe array was exposed to 10 washes in 6× SSPE-T at 25 °C followed by 4 washes in 0.5× SSPE-T at 50 °C. The biotinylated cRNA was stained with a streptavidin-phycoerythrin conjugate, 10 μg/ml (Molecular Probes) in 6× SSPE-T

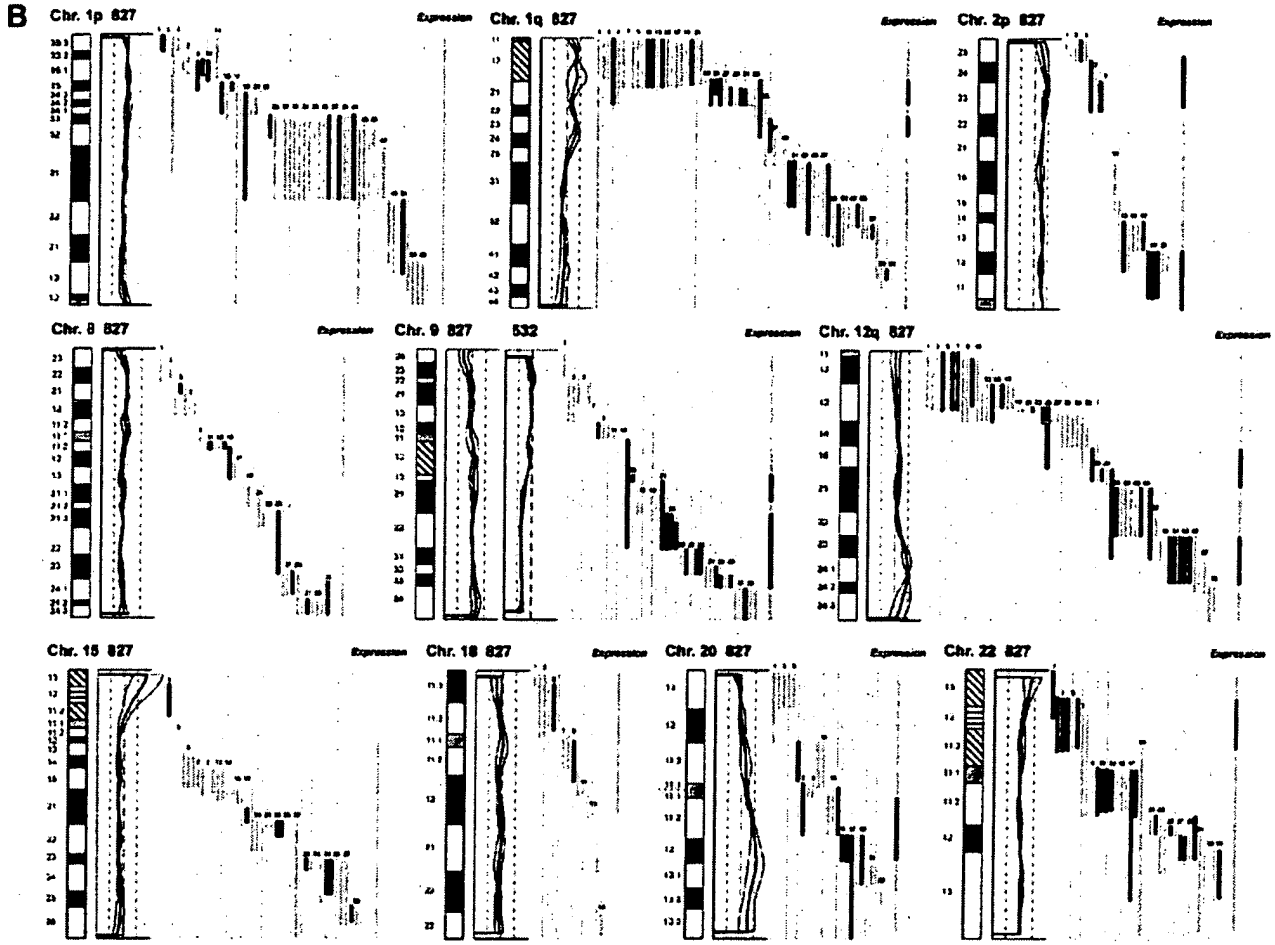

FIG. 1—*continued*

for 30 min at 25 °C followed by 10 washes in 6× SSPE-T at 25 °C. The probe arrays were scanned at 560 nm using a confocal laser scanning microscope (made for Affymetrix by Hewlett-Packard). The readings from the quantitative scanning were analyzed by Affymetrix gene expression analysis software.

Microsatellite Analysis—Microsatellite Analysis was performed as described previously (14). Microsatellites were selected by use of www.ncbi.nlm.nih.gov/genemap98, and primer sequences were obtained from the genome data base at www.gdb.org. DNA was extracted from tumor and blood and amplified by PCR in a volume of 20 μl for 35 cycles. The amplicons were denatured and electrophoresed for 3 h in an ABI Prism 377. Data were collected in the Gene Scan program for fragment analysis. Loss of heterozygosity was defined as less than 33% of one allele detected in tumor amplicons compared with blood.

Proteomic Analysis—TCCs were minced into small pieces and homogenized in a small glass homogenizer in 0.5 ml of lysis solution. Samples were stored at −20 °C until use. The procedure for 2D gel electrophoresis has been described in detail elsewhere (15, 16). Gels were stained with silver nitrate and/or Coomassie Brilliant Blue. Proteins were identified by a combination of procedures that included microsequencing, mass spectrometry, two-dimensional gel Western immunoblotting, and comparison with the master two-dimensional gel image of human keratinocyte proteins; see biobase.dk/cgi-bin/celis.

CGH—Hybridization of differentially labeled tumor and normal DNA to normal metaphase chromosomes was performed as described previously (10). Fluorescein-labeled tumor DNA (200 ng), Texas Red-labeled reference DNA (200 ng), and human Cot-1 DNA (20 μg) were denatured at 37 °C for 5 min and applied to denatured normal metaphase slides. Hybridization was at 37 °C for 2 days. After washing, the slides were counterstained with 0.15 μg/ml 4,6-diamidino-2-phenylindole in an anti-fade solution. A second hybridization was performed for all tumor samples using fluorescein-labeled reference DNA and Texas Red-labeled tumor DNA (inverse labeling) to confirm the aberrations detected during the initial hybridization. Each CGH experiment also included a normal control hybridization using fluorescein- and Texas Red-labeled normal DNA. Digital image analysis was used to identify chromosomal regions with abnormal fluorescence ratios, indicating regions of DNA gains and losses. The average green:red fluorescence intensity ratio profiles were calculated using four images of each chromosome (eight chromosomes total) with normalization of the green:red fluorescence intensity ratio for the entire metaphase and background correction. Chromosome identification was performed based on 4,6-diamidino-2-phenylindole banding patterns. Only images showing uniform high intensity fluorescence with minimal background staining were analyzed. All centromeres, p arms of acrocentric chromosomes, and heterochromatic regions were excluded from the analysis.

RESULTS

Comparative Genomic Hybridization—The CGH analysis identified a number of chromosomal gains and losses in the

TABLE I

Correlation between alterations detected by CGH and by expression monitoring

Top, CGH used as independent variable (if CGH alteration – what expression ratio was found); bottom, altered expression used as independent variable (if expression alteration – what CGH deviation was found).

CGH alterations	Tumor 733 vs. 335 Expression change clusters	Concordance	CGH alterations	Tumor 827 vs. 532 Expression change clusters	Concordance
13 Gain	10 Up-regulation 0 Down-regulation 3 No change	77%	10 Gain	8 Up-regulation 0 Down-regulation 2 No change	80%
10 Loss	1 Up-regulation 5 Down-regulation 4 No change	50%	12 Loss	3 Up-regulation 2 Down regulation 7 No change	17%

Expression change clusters	Tumor 733 vs. 335 CGH alterations	Concordance	Expression change clusters	Tumor 827 vs. 532 CGH alterations	Concordance
16 Up-regulation	11 Gain 2 Loss 3 No change	69%	17 Up-regulation	10 Gain 5 Loss 2 No change	59%
21 Down-regulation	1 Gain 8 Loss 12 No change	38%	9 Down-regulation	0 Gain 3 Loss 6 No change	33%
15 No change	3 Gain 3 Loss 9 No change	60%	21 No change	1 Gain 3 Loss 17 No change	81%

two invasive tumors (stage pT1, TCCs 733 and 827), whereas the two non-invasive papillomas (stage pTa, TCCs 335 and 532) showed only 9p−, 9q22-q33−, and X−, and 7+, 9q−, and Y−, respectively. Both invasive tumors showed changes (1q22–24+, 2q14.1-qter−, 3q12-q13.3−, 6q12-q22−, 9q34+, 11q12-q13+, 17+, and 20q11.2-q12+) that are typical for their disease stage, as well as additional alterations, some of which are shown in Fig. 1. Areas with gains and losses deviated from the normal copy number to some extent, and the average numerical deviation from normal was 0.4-fold in the case of TCC 733 and 0.3-fold for TCC 827. The largest changes, amounting to at least a doubling of chromosomal content, were observed at 1q23 in TCC 733 (Fig. 1*A*) and 20q12 in TCC 827 (Fig. 1*B*).

mRNA Expression in Relation to DNA Copy Number—The mRNA levels from the two invasive tumors (TCCs 827 and 733) were compared with the two non-invasive counterparts (TCCs 532 and 335). This was done in two separate experiments in which we compared TCCs 733 to 335 and 827 to 532, respectively, using two different scaling settings for the arrays to rule out scaling as a confounding parameter. Approximately 1,800 genes that yielded a signal on the arrays were searched in the Unigene and Genemap data bases for chromosomal location, and those with a known location (1096) were plotted as bars covering their purported locus. In that way it was possible to construct a graphic presentation of DNA copy number and relative mRNA levels along the individual chromosomes (Fig. 1).

For each mRNA a ratio was calculated between the level in the invasive *versus* the non-invasive counterpart. Bars, which represent chromosomal location of a gene, were color-coded according to the expression ratio, and only differences larger than 2-fold were regarded as informative (Fig. 1). The density of genes along the chromosomes varied, and areas containing only one gene were excluded from the calculations. The resolution of the CGH method is very low, and some of the outlier data may be because of the fact that the boundaries of the chromosomal aberrations are not known at high resolution.

Two sets of calculations were made from the data. For the first set we used CGH alterations as the independent variable and estimated the frequency of expression alterations in these chromosomal areas. In general, areas with a strong gain of chromosomal material contained a cluster of genes having increased mRNA expression. For example, both chromosomes 1q21-q25, 2p and 9q, showed a relative gain of more than 100% in DNA copy number that was accompanied by increased mRNA expression levels in the two tumor pairs (Fig. 1). In most cases, chromosomal gains detected by CGH were accompanied by an increased level of transcripts in both TCCs 733 (77%) and 827 (80%) (Table I, *top*). Chromosomal losses, on the other hand, were not accompanied by decreased expression in several cases, and were often registered as having unaltered RNA levels (Table I, *top*). The inability to detect RNA expression changes in these cases was not because of fewer genes mapping to the lost regions (data not shown).

In the second set of calculations we selected expression alterations above 2-fold as the independent variable and estimated the frequency of CGH alterations in these areas. As above, we found that increased transcript expression correlated with gain of chromosomal material (TCC 733, 69% and TCC 827, 59%), whereas reduced expression was often detected in areas with unaltered CGH ratios (Table I, *bottom*). Furthermore, as a control we looked at areas with no alter-

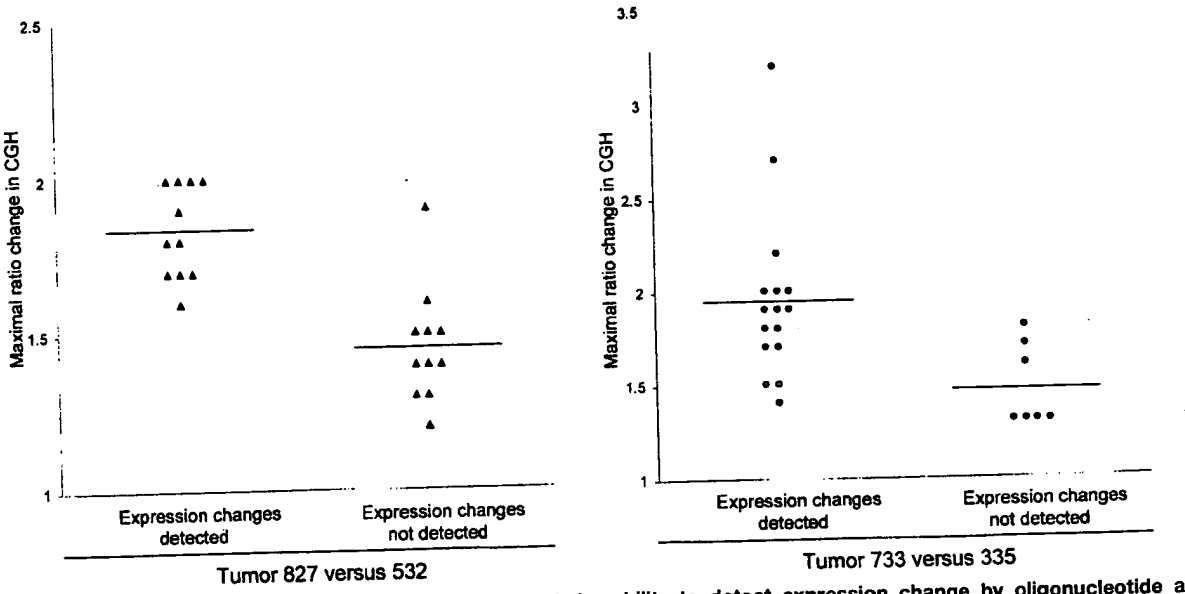

FIG. 2. **Correlation between maximum CGH aberration and the ability to detect expression change by oligonucleotide array monitoring.** The aberration is shown as a numerical -fold change in ratio between invasive tumors 827 (▲) and 733 (♦) and their non-invasive counterparts 532 and 335. The expression change was taken from the *Expression* line to the *right* in Fig. 1, which depicts the resulting expression change for a given chromosomal region. At least half of the mRNAs from a given region have to be either up- or down-regulated to be scored as an expression change. All chromosomal arms in which the CGH ratio plus or minus one standard deviation was outside the ratio value of one were included.

ation in expression. No alteration was detected by CGH in most of these areas (TCC 733, 60% and TCC 827, 81%; see Table I, *bottom*). Because the ability to observe reduced or increased mRNA expression clustering to a certain chromosomal area clearly reflected the extent of copy number changes, we plotted the maximum CGH aberrations in the regions showing CGH changes against the ability to detect a change in mRNA expression as monitored by the oligonucleotide arrays (Fig. 2). For both tumors TCC 733 ($p < 0.015$) and TCC 827 ($p < 0.00003$) a highly significant correlation was observed between the level of CGH ratio change (reflecting the DNA copy number) and alterations detected by the array based technology (Fig. 2). Similar data were obtained when areas with altered expression were used as independent variables. These areas correlated best with CGH when the CGH ratio deviated 1.6- to 2.0-fold (Table I, *bottom*) but mostly did not at lower CGH deviations. These data probably reflect that loss of an allele may only lead to a 50% reduction in expression level, which is at the cut-off point for detection of expression alterations. Gain of chromosomal material can occur to a much larger extent.

Microsatellite-based Detection of Minor Areas of Losses—In TCC 733, several chromosomal areas exhibiting DNA amplification were preceded or followed by areas with a normal CGH but reduced mRNA expression (see Fig. 1, TCC 733 chromosome 1q32, 2p21, and 7q21 and q32, 9q34, and 10q22). To determine whether these results were because of undetected loss of chromosomal material in these regions or because of other non-structural mechanisms regulating transcription, we examined two microsatellites positioned at chromosome 1q25–32 and two at chromosome 2p22. Loss of heterozygosity (LOH) was found at both 1q25 and at 2p22 indicating that minor deleted areas were not detected with the resolution of CGH (Fig. 3). Additionally, chromosome 2p in TCC 733 showed a CGH pattern of gain/no change/gain of DNA that correlated with transcript increase/decrease/increase. Thus, for the areas showing increased expression there was a correlation with the DNA copy number alterations (Fig. 1*A*). As indicated above, the mRNA decrease observed in the middle of the chromosomal gain was because of LOH, implying that one of the mechanisms for mRNA down-regulation may be regions that have undergone smaller losses of chromosomal material. However, this cannot be detected with the resolution of the CGH method.

In both TCC 733 and TCC 827, the telomeric end of chromosome 11p showed a normal ratio in the CGH analysis; however, clusters of five and three genes, respectively, lost their expression. Two microsatellites (D11S1760, D11S922) positioned close to MUC2, IGF2, and cathepsin D indicated LOH as the most likely mechanism behind the loss of expression (data not shown).

A reduced expression of mRNA observed in TCC 733 at chromosomes 3q24, 11p11, 12p12.2, 12q21.1, and 16q24 and in TCC 827 at chromosome 11p15.5, 12p11, 15q11.2, and 18q12 was also examined for chromosomal losses using microsatellites positioned as close as possible to the gene loci

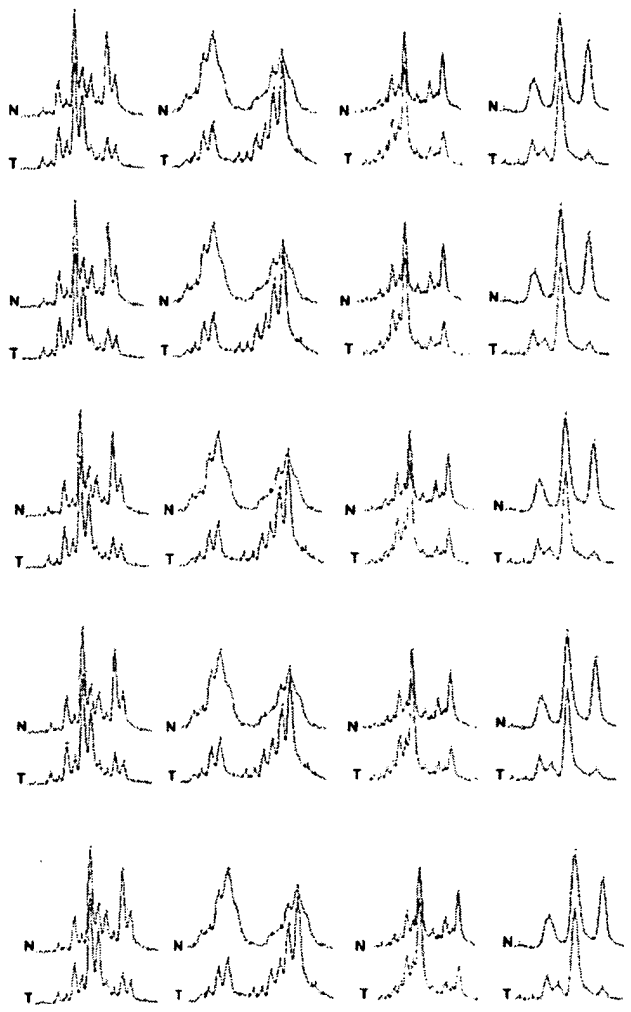

FIG. 3. **Microsatellite analysis of loss of heterozygosity.** Tumor 733 showing loss of heterozygosity at chromosome 1q25, detected (*a*) by D1S215 close to Hu class I histocompatibility antigen (gene number 38 in Fig. 1), (*b*) by D1S2735 close to cathepsin E (gene number 41 in Fig. 1), and (*c*) at chromosome 2p23 by D2S2251 close to general β-spectrin (gene number 11 on Fig. 1) and of (*d*) tumor 827 showing loss of heterozygosity at chromosome 18q12 by S18S1118 close to mitochondrial 3-oxoacyl-coenzyme A thiolase (gene number 12 in Fig. 1). The *upper curves* show the electropherogram obtained from normal DNA from leukocytes (*N*), and the *lower curves* show the electropherogram from tumor DNA (*T*). In all cases one allele is partially lost in the tumor amplicon.

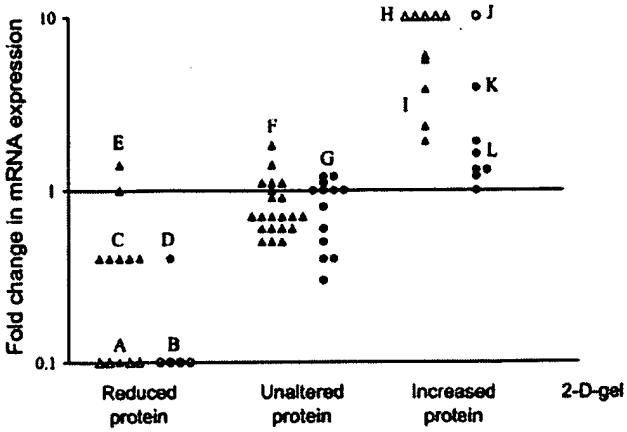

FIG. 4. **Correlation between protein levels as judged by 2D-PAGE and transcript ratio.** For comparison proteins were divided in three groups, unaltered in level or up- or down-regulated (*horizontal axis*). The mRNA ratio as determined by oligonucleotide arrays was plotted for each gene (*vertical axis*). ▲, mRNAs that were scored as present in both tumors used for the ratio calculation; △, mRNAs that were scored as absent in the invasive tumors (along *horizontal axis*) or as absent in non-invasive reference (*top* of figure). Two different scalings were used to exclude scaling as a confounder, TCCs 827 and 532 (▲△) were scaled with background suppression, and TCCs 733 and 335 (●○) were scaled without suppression. Both comparisons showed highly significant ($p < 0.005$) differences in mRNA ratios between the groups. Proteins shown were as follows: Group *A* (from *left*), phosphoglucomutase 1, glutathione transferase class μ number 4, fatty acid-binding protein homologue, cytokeratin 15, and cytokeratin 13; *B* (from *left*), fatty acid-binding protein homologue, 28-kDa heat shock protein, cytokeratin 13, and calcyclin; *C* (from *left*), α-enolase, hnRNP B1, 28-kDa heat shock protein, 14–3-3-ε, and pre-mRNA splicing factor; *D*, mesothelial keratin K7 (type II); *E* (from *top*), glutathione *S*-transferase-π and mesothelial keratin K7 (type II); *F* (from *top* and *left*), adenylyl cyclase-associated protein, E-cadherin, keratin 19, calgizzarin, phosphoglycerate mutase, annexin IV, cytoskeletal γ-actin, hnRNP A1, integral membrane protein calnexin (IP90), hnRNP H, brain-type clathrin light chain-a, hnRNP F, 70-kDa heat shock protein, heterogeneous nuclear ribonucleoprotein A/B, translationally controlled tumor protein, liver glyceraldehyde-3-phosphate dehydrogenase, keratin 8, aldehyde reductase, and Na,K-ATPase β-1 subunit; *G*, (from *top* and *left*), TCP20, calgizzarin, 70-kDa heat shock protein, calnexin, hnRNP H, cytokeratin 15, ATP synthase, keratin 19, triosephosphate isomerase, hnRNP F, liver glyceraldehyde-3-phosphatase dehydrogenase, glutathione *S*-transferase-π, and keratin 8; *H* (from *left*), plasma gelsolin, autoantigen calreticulin, thioredoxin, and NAD+-dependent 15 hydroxyprostaglandin dehydrogenase; *I* (from *top*), prolyl 4-hydroxylase β-subunit, cytokeratin 20, cytokeratin 17, prohibition, and fructose 1,6-biphosphatase; *J* annexin II; *K*, annexin IV; *L* (from *top* and *left*), 90-kDa heat shock protein, prolyl 4-hydroxylase β-subunit, α-enolase, GRP 78, cyclophilin, and cofilin.

showing reduced mRNA transcripts. Only the microsatellite positioned at 18q12 showed LOH (Fig. 3), suggesting that transcriptional down-regulation of genes in the other regions may be controlled by other mechanisms.

Relation between Changes in mRNA and Protein Levels—2D-PAGE analysis, in combination with Coomassie Brilliant Blue and/or silver staining, was carried out on all four tumors using fresh biopsy material. 40 well resolved abundant known proteins migrating in areas away from the edges of the pH gradient, and having a known chromosomal location, were selected for analysis in the TCC pair 827/532. Proteins were identified by a combination of methods (see "Experimental Procedures"). In general there was a highly significant correlation ($p < 0.005$) between mRNA and protein alterations (Fig. 4). Only one gene showed disagreement between transcript alteration and protein alteration. Except for a group of cyto-

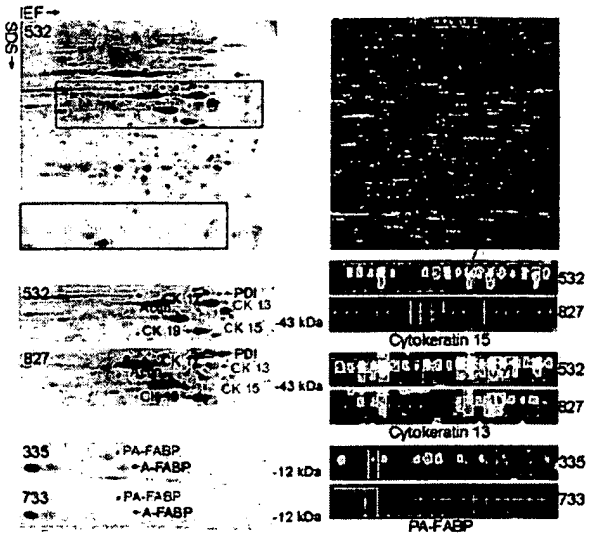

FIG. 5. **Comparison of protein and transcript levels in invasive and non-invasive TCCs.** The *upper part* of the figure shows a 2D gel (*left*) and the oligonucleotide array (*right*) of TCC 532. The *red rectangles* on the *upper gel* highlight the areas that are compared below. Identical areas of 2D gels of TCCs 532 and 827 are shown below. Clearly, cytokeratins 13 and 15 are strongly down-regulated in TCC 827 (*red annotation*). The tile on the array containing probes for cytokeratin 15 is enlarged *below* the array (*red arrow*) from TCC 532 and is compared with TCC 827. The *upper row* of *squares* in each tile corresponds to perfect match probes; the *lower row* corresponds to mismatch probes containing a mutation (used for correction for unspecific binding). Absence of signal is depicted as *black*, and the higher the signal the lighter the color. A high transcript level was detected in TCC 532 (6151 units) whereas a much lower level was detected in TCC 827 (absence of signals). For cytokeratin 13, a high transcript level was also present in TCC 532 (15659 units), and a much lower level was present in TCC 827 (623 units). The 2D gels at the *bottom* of the figure (*left*) show levels of PA-FABP and adipocyte-FABP in TCCs 335 and 733 (invasive), respectively. Both proteins are down-regulated in the invasive tumor. To the *right* we show the array tiles for the PA-FABP transcript. A medium transcript level was detected in the case of TCC 335 (1277 units) whereas very low levels were detected in TCC 733 (166 units). *IEF*, isoelectric focusing.

keratins encoded by genes on chromosome 17 (Fig. 5) the analyzed proteins did not belong to a particular family. 26 well focused proteins whose genes had a know chromosomal location were detected in TCCs 733 and 335, and of these 19 correlated ($p < 0.005$) with the mRNA changes detected using the arrays (Fig. 4). For example, PA-FABP was highly expressed in the non-invasive TCC 335 but lost in the invasive counterpart (TCC 733; see Fig. 5). The smaller number of proteins detected in both 733 and 335 was because of the smaller size of the biopsies that were available.

11 chromosomal regions where CGH showed aberrations that corresponded to the changes in transcript levels also showed corresponding changes in the protein level (Table II). These regions included genes that encode proteins that are found to be frequently altered in bladder cancer, namely cytokeratins 17 and 20, annexins II and IV, and the fatty acid-binding proteins PA-FABP and FBP1. Four of these proteins were encoded by genes in chromosome 17q, a frequently amplified chromosomal area in invasive bladder cancers.

DISCUSSION

Most human cancers have abnormal DNA content, having lost some chromosomal parts and gained others. The present study provides some evidence as to the effect of these gains and losses on gene expression in two pairs of non-invasive and invasive TCCs using high throughput expression arrays and proteomics, in combination with CGH. In general, the results showed that there is a clear individual regulation of the mRNA expression of single genes, which in some cases was superimposed by a DNA copy number effect. In most cases, genes located in chromosomal areas with gains often exhibited increased mRNA expression, whereas areas showing losses showed either no change or a reduced mRNA expression. The latter might be because of the fact that losses most often are restricted to loss of one allele, and the cut-off point for detection of expression alterations was a 2-fold change, thus being at the border of detection. In several cases, how-

TABLE II
Proteins whose expression level correlates with both mRNA and gene dose changes

Protein	Chromosomal location	Tumor TCC	CGH alteration	Transcript alteration[a]	Protein alteration
Annexin II	1q21	733	Gain	Abs to Pres[a]	Increase
Annexin IV	2p13	733	Gain	3.9-Fold up	Increase
Cytokeratin 17	17q12-q21	827	Gain	3.8-Fold up	Increase
Cytokeratin 20	17q21.1	827	Gain	5.6-Fold up	Increase
(PA-)FABP	8q21.2	827	Loss	10-Fold down	Decrease
FBP1	9q22	827	Gain	2.3-Fold up	Increase
Plasma gelsolin	9q31	827	Gain	Abs to Pres	Increase
Heat shock protein 28	15q12-q13	827	Loss	2.5-Fold up	Decrease
Prohibitin	17q21	827/733	Gain	3.7-/2.5-Fold up[b]	Increase
Prolyl-4-hydroxyl	17q25	827/733	Gain	5.7-/1.6-Fold up	Increase
hnRNPB1	7p15	827	Loss	2.5-Fold down	Decrease

[a] Abs, absent; Pres, present.
[b] In cases where the corresponding alterations were found in both TCCs 827 and 733 these are shown as 827/733.

ever, an increase or decrease in DNA copy number was associated with *de novo* occurrence or complete loss of transcript, respectively. Some of these transcripts could not be detected in the non-invasive tumor but were present at relatively high levels in areas with DNA amplifications in the invasive tumors (*e.g.* in TCC 733 transcript from cellular ligand of annexin II gene (chromosome 1q21) from absent to 2670 arbitrary units; in TCC 827 transcript from small proline-rich protein 1 gene (chromosome 1q12-q21.1) from absent to 1326 arbitrary units). It may be anticipated from these data that significant clustering of genes with an increased expression to a certain chromosomal area indicates an increased likelihood of gain of chromosomal material in this area.

Considering the many possible regulatory mechanisms acting at the level of transcription, it seems striking that the gene dose effects were so clearly detectable in gained areas. One hypothetical explanation may lie in the loss of controlled methylation in tumor cells (17–19). Thus, it may be possible that in chromosomes with increased DNA copy numbers two or more alleles could be demethylated simultaneously leading to a higher transcription level, whereas in chromosomes with losses the remaining allele could be partly methylated, turning off the process (20, 21). A recent report has documented a ploidy regulation of gene expression in yeast, but in this case all the genes were present in the same ratio (22), a situation that is not analogous to that of cancer cells, which show marked chromosomal aberrations, as well as gene dosage effects.

Several CGH studies of bladder cancer have shown that some chromosomal aberrations are common at certain stages of disease progression, often occurring in more than 1 of 3 tumors. In pTa tumors, these include 9p−, 9q−, 1q+, Y− (2, 6), and in pT1 tumors, 2q−,11p−, 11q−, 1q+, 5p+, 8q+, 17q+, and 20q+ (2–4, 6, 7). The pTa tumors studied here showed similar aberrations such as 9p− and 9q22-q33− and 9q− and Y−, respectively. Likewise, the two minimal invasive pT1 tumors showed aberrations that are commonly seen at that stage, and TCC 827 had a remarkable resemblance to the commonly seen pattern of losses and gains, such as 1q22–24 amplification (seen in both tumors), 11q14-q22 loss, the latter often linked to 17 q+ (both tumors), and 1q+ and 9p−, often linked to 20q+ and 11 q13+ (both tumors) (7–9). These observations indicate that the pairs of tumors used in this study exhibit chromosomal changes observed in many tumors, and therefore the findings could be of general importance for bladder cancer.

Considering that the mapping resolution of CGH is of about 20 megabases it is only possible to get a crude picture of chromosomal instability using this technique. Occasionally, we observed reduced transcript levels close to or inside regions with increased copy numbers. Analysis of these regions by positioning heterozygous microsatellites as close as possible to the locus showing reduced gene expression revealed loss of heterozygosity in several cases. It seems likely that multiple and different events occur along each chromosomal arm and that the use of cDNA microarrays for analysis of DNA copy number changes will reach a resolution that can resolve these changes, as has recently been proposed (2). The outlier data were not more frequent at the boundaries of the CGH aberrations. At present we do not know the mechanism behind chromosomal aneuploidy and cannot predict whether chromosomal gains will be transcribed to a larger extent than the two native alleles. A mechanism as genetic imprinting has an impact on the expression level in normal cells and is often reduced in tumors. However, the relation between imprinting and gain of chromosomal material is not known.

We regard it as a strength of this investigation that we were able to compare invasive tumors to benign tumors rather than to normal urothelium, as the tumors studied were biologically very close and probably may represent successive steps in the progression of bladder cancer. Despite the limited amount of fresh tissue available it was possible to apply three different state of the art methods. The observed correlation between DNA copy number and mRNA expression is remarkable when one considers that different pieces of the tumor biopsies were used for the different sets of experiments. This indicate that bladder tumors are relatively homogenous, a notion recently supported by CGH and LOH data that showed a remarkable similarity even between tumors and distant metastasis (10, 23).

In the few cases analyzed, mRNA and protein levels showed a striking correspondence although in some cases we found discrepancies that may be attributed to translational regulation, post-translational processing, protein degradation, or a combination of these. Some transcripts belong to undertranslated mRNA pools, which are associated with few translationally inactive ribosomes; these pools, however, seem to be rare (24). Protein degradation, for example, may be very important in the case of polypeptides with a short half-life (*e.g.* signaling proteins). A poor correlation between mRNA and protein levels was found in liver cells as determined by arrays and 2D-PAGE (25), and a moderate correlation was recently reported by Ideker *et al.* (26) in yeast.

Interestingly, our study revealed a much better correlation between gained chromosomal areas and increased mRNA levels than between loss of chromosomal areas and reduced mRNA levels. In general, the level of CGH change determined the ability to detect a change in transcript. One possible explanation could be that by losing one allele the change in mRNA level is not so dramatic as compared with gain of material, which can be rather unlimited and may lead to a severalfold increase in gene copy number resulting in a much higher impact on transcript level. The latter would be much easier to detect on the expression arrays as the cut-off point was placed at a 2-fold level so as not to be biased by noise on the array. Construction of arrays with a better signal to noise ratio may in the future allow detection of lesser than 2-fold alterations in transcript levels, a feature that may facilitate the analysis of the effect of loss of chromosomal areas on transcript levels.

In eleven cases we found a significant correlation between DNA copy number, mRNA expression, and protein level. Four of these proteins were encoded by genes located at a frequently amplified area in chromosome 17q. Whether DNA copy number is one of the mechanisms behind alteration of these eleven proteins is at present unknown and will have to be proved by other methods using a larger number of samples. One factor making such studies complicated is the large extent of protein modification that occurs after translation, requiring immunoidentification and/or mass spectrometry to correctly identify the proteins in the gels.

In conclusion, the results presented in this study exemplify the large body of knowledge that may be possible to gather in the future by combining state of the art techniques that follow the pathway from DNA to protein (26). Here, we used a traditional chromosomal CGH method, but in the future high resolution CGH based on microarrays with many thousand radiation hybrid-mapped genes will increase the resolution and information derived from these types of experiments (2). Combined with expression arrays analyzing transcripts derived from genes with known locations, and 2D gel analysis to obtain information at the post-translational level, a clearer and more developed understanding of the tumor genome will be forthcoming.

Acknowledgments—We thank Mie Madsen, Hanne Steen, Inge Lis Thorsen, Hans Lund, Vikolaj Ørntoft, and Lynn Bjerke for technical help and Thomas Gingeras, Christine Harrington, and Morten Østergaard for valuable discussions.

* This work was supported by grants from The Danish Cancer Society, the University of Aarhus, Aarhus County, Novo Nordic, the Danish Biotechnology Program, the Frenkels Foundation, the John and Birthe Meyer Foundation, and NCI, National Institutes of Health Grant CA47537. The costs of publication of this article were defrayed in part by the payment of page charges. This article must therefore be hereby marked "*advertisement*" in accordance with 18 U.S.C. Section 1734 solely to indicate this fact.

§ To whom correspondence should be addressed: Dept. of Clinical Biochemistry, Molecular Diagnostic Laboratory, Aarhus University Hospital, Skejby, DK-8200 Aarhus N, Denmark. Tel.: 45-89495100/45-86156201 (private); Fax: 45-89496018; E-mail: orntoft@kba.sks.au.dk.

REFERENCES

1. Lengauer, C., Kinzler, K. W., and Vogelstein, B. (1998) Genetic instabilities in human cancers. *Nature* **17,** 643–649
2. Pollack, J. R., Perou, C. M., Alizadeh, A. A., Eisen, M. B., Pergamenschikov, A., Williams, C. F., Jeffrey, S. S., Botstein, D., and Brown, P. O. (1999) Genome-wide analysis of DNA copy-number changes using cDNA microarrays. *Nat. Genet.* **23,** 41–46
3. de Cremoux, P., Martin, E. C., Vincent-Salomon, A., Dieras, V., Barbaroux, C., Liva, S., Pouillart, P., Sastre-Garau, X., and Magdelenat, H. (1999) Quantitative PCR analysis of c-erb B-2 (HER2/neu) gene amplification and comparison with p185(HER2/neu) protein expression in breast cancer drill biopsies. *Int. J. Cancer* **83,** 157–161
4. Brungier, P. P., Tamimi, Y., Shuuring, E., and Schalken, J. (1996) Expression of cyclin D1 and EMS1 in bladder tumors; relationship with chromosome 11q13 amplifications. *Oncogene* **12,** 1747–1753
5. Slavc, I., Ellenbogen, R., Jung, W. H., Vawter, G. F., Kretschmar, C., Grier, H., and Korf, B. R. (1990) *myc* gene amplification and expression in primary human neuroblastoma. *Cancer Res.* **50,** 1459–1463
6. Sauter, G., Carroll, P., Moch, H., Kallioniemi, A., Kerschmann, R., Narayan, P., Mihatsch, M. J., and Waldman, F. M. (1995) c-*myc* copy number gains in bladder cancer detected by fluorescence *in situ* hybridization. *Am J. Pathol.* **146,** 1131–1139
7. Richter, J., Jiang, F., Gorog, J. P., Sartorious, G., Egenter, C., Gasser, T. C., Moch, H., Mihatsch, M. J., and Sauter, G. (1997) Marked genetic differences between stage pTa and stage pT1 papillary bladder cancer detected by comparative genomic hybridization. *Cancer Res.* **57,** 2860–2864
8. Richter, J., Beffa, L., Wagner, U., Schraml, P., Gasser, T. C., Moch, H., Mihatsch, M. J., and Sauter, G. (1998) Patterns of chromosomal imbalances in advanced urinary bladder cancer detected by comparative genomic hybridization. *Am. J. Pathol.* **153,** 1615–1621
9. Bruch, J., Wohr, G., Hautmann, R., Mattfeldt, T., Bruderlein, S., Moller, P., Sauter, S., Hameister, H., Vogel, W., and Paiss, T. (1998) Chromosomal changes during progression of transitional cell carcinoma of the bladder and delineation of the amplified interval on chromosome arm 8q. *Genes Chromosomes Cancer* **23,** 167–174
10. Hovey, R. M., Chu, L., Balazs, M., De Vries, S., Moore, D., Sauter, G., Carroll, P. R., and Waldman, F. M. (1998) Genetic alterations in primary bladder cancers and their metastases. *Cancer Res.* **15,** 3555–3560
11. Simon, R., Burger, H., Brinkschmidt, C., Bocker, W., Hertle, L., and Terpe, H. J. (1998) Chromosomal aberrations associated with invasion in papillary superficial bladder cancer. *J. Pathol.* **185,** 345–351
12. Koo, S. H., Kwon, K. C., Ihm, C. H., Jeon, Y. M., Park, J. W., and Sul, C. K. (1999) Detection of genetic alterations in bladder tumors by comparative genomic hybridization and cytogenetic analysis. *Cancer Genet. Cytogenet.* **110,** 87–93
13. Wodicka, L., Dong, H., Mittmann, M., Ho, M. H., and Lockhart, D. J. (1997) Genome-wide expression monitoring in *Saccharomyces cerevisiae*. *Nat. Biotechnol.* **15,** 1359–1367
14. Christensen, M., Sunde, L., Bolund, L., and Orntoft, T. F. (1999) Comparison of three methods of microsatellite detection. *Scand. J. Clin. Lab. Invest.* **59,** 167–177
15. Celis, J. E., Ostergaard, M., Basse, B., Celis, A., Lauridsen, J. B., Ratz, G. P., Andersen, I., Hein, B., Wolf, H., Orntoft, T. F., and Rasmussen, H. H. (1996) Loss of adipocyte-type fatty acid binding protein and other protein biomarkers is associated with progression of human bladder transitional cell carcinomas. *Cancer Res.* **56,** 4782–4790
16. Celis, J. E., Ratz, G., Basse, B., Lauridsen, J. B., and Celis, A. (1994) in *Cell Biology: A Laboratory Handbook* (Celis, J. E., ed) Vol. 3, pp. 222–230, Academic Press, Orlando, FL
17. Ohlsson, R., Tycko, B., and Sapienza, C. (1998) Monoallelic expression: 'there can only be one'. *Trends Genet.* **14,** 435–438
18. Hollander, G. A., Zuklys, S., Morel, C., Mizoguchi, E., Mobisson, K., Simpson, S., Terhorst, C., Wishart, W., Golan, D. E., Bhan, A. K., and Burakoff, S. J. (1998) Monoallelic expression of the interleukin-2 locus. *Science* **279,** 2118–2121
19. Brannan, C. I., and Bartolomei, M. S. (1999) Mechanisms of genomic imprinting. *Curr. Opin. Genet. Dev.* **9,** 164–170
20. Ohlsson, R., Cui, H., He, L., Pfeifer, S., Malmikumpa, H., Jiang, S., Feinberg, A. P., and Hedborg, F. (1999) Mosaic allelic insulin-like growth factor 2 expression patterns reveal a link between Wilms' tumorigenesis and epigenetic heterogeneity. *Cancer Res.* **59,** 3889–3892
21. Cui, H., Hedborg, F., He, L., Nordenskjold, A., Sandstedt, B., Pfeifer-Ohlsson, S., and Ohlsson, R. (1997) Inactivation of H19, an imprinted and putative tumor repressor gene, is a preneoplastic event during Wilms' tumorigenesis. *Cancer Res.* **57,** 4469–4473
22. Galitski, T., Saldanha, A. J., Styles, C. A., Lander, E. S., and Fink, G. R. (1999) Ploidy regulation of gene expression. *Science* **285,** 251–254
23. Tsao, J., Yatabe, Y., Markl, I. D., Hajyan, K., Jones, P. A., and Shibata, D. (2000) Bladder cancer genotype stability during clinical progression. *Genes Chromosomes Cancer* **29,** 26–32
24. Zong, Q., Schummer, M., Hood, L., and Morris, D. R. (1999) Messenger RNA translation state: the second dimension of high-throughput expression screening. *Proc. Natl. Acad. Sci. U. S. A.* **96,** 10632–10636
25. Anderson, L., and Seilhamer, J. (1997) Comparison of selected mRNA and protein abundances in human liver. *Electrophoresis* **18,** 533–537
26. Ideker, T., Thorsson, V., Ranish, J. A., Christmas, R., Buhler, J., Eng, J. K., Bumgarner, R., Goodlett, D. R., Aebersold, R., and Hood, L. (2001) Integrated genomic and proteomic analyses of a systematically perturbed metabolic network. *Science* **292,** 929–934

PAGE4 Is a Cytoplasmic Protein That Is Expressed in Normal Prostate and in Prostate Cancers

Carlo Iavarone, Curt Wolfgang,[1] Vasantha Kumar, Paul Duray, Mark Willingham, Ira Pastan, and Tapan K. Bera[2]

Laboratory of Molecular Biology [C. I., C. W., V. K., I. P., T. K. B.], and of Pathology [P. D.], Clinical Cancer Research, National Cancer Institute, NIH, Bethesda, Maryland 20892, and Department of Pathology, Wake Forest University School of Medicine, Winston-Salem, North Carolina 27157 [M. W.]

Abstract

***PAGE4* is an X chromosome-linked cancer-testis antigen that was identified by expressed sequence tags database mining and a functional genomic approach. *PAGE4* is preferentially expressed in normal male and female reproductive tissues and also in a variety of cancers including prostate. In the present study, we have used *in situ* hybridization to show that *PAGE4* mRNA is expressed only in the epithelial cells of normal and prostate-cancer specimens. Analysis of the protein product encoded by the *PAGE4* mRNA reveals that it encodes a M_r 16,000 protein and is detected in tissue extracts from both normal prostate and prostate cancer. Cell fractionation analysis of PAGE4 protein indicates that PAGE4 is localized in the cytoplasm of the cell. Furthermore, cDNA microarray analysis indicates that the expression of *lipoprotein lipase*, a gene frequently deleted in prostate cancer, is down-regulated in a cell line that expresses *PAGE4*.**

Introduction

Prostate cancer is a major public health problem and the second leading cause of death for men in the United States. About one in five men in the United States will develop prostate cancer during their lifetime. Despite its distinction as the most frequently diagnosed noncutaneous cancer, little is known about the causes of this disease largely because of the cellular heterogeneity of the prostate and the lack of systematic analysis of the genes expressed in this tissue. Completion of the human genome project and the technological advancement in biomedical research has enabled researchers to identify and to systematically analyze new genes that could be used as targets for cancer therapy or that could be involved in the multistep process of cancer. Many different methods are currently being used to identify tissue- or cancer-specific genes. Our laboratory is interested in identifying genes by using the EST[3] database, and developed a computer-based screening strategy to generate clusters of ESTs that are specifically expressed in normal prostate and/or prostate cancer but not in essential normal tissues (1). We then used experimental approaches to verify these predictions. Using this approach, we identified *PAGE4*, a new gene expressed in normal prostate and testis and highly expressed in prostate and uterine cancers (2).

In this report, we analyzed *PAGE4* mRNA expression by *in situ* hybridization using several prostate cancer samples. We also report here the characterization and subcellular localization of the protein encoded by *PAGE4* mRNA. Using cell fractionation and immunofluorescence analysis we demonstrate that the M_r 16,000 protein product of *PAGE4* is localized in the cytoplasm of the cell. In addition, using cDNA microarray analysis, we report that the expression of *LPL*, a gene involved in lipid metabolism, is down-regulated in cells expressing *PAGE4*.

Materials and Methods

Primers. Nucleotide sequences of the primers used in this study were: forward CP1 (5′-AAGAGGAATTCGCAGCGATGAGTGCACGA-3′), and reverse CP2 (5′-GCACTGAATTCTCAGCCATGTGTGTAGCT-′); forward CR1 (5′-AAGAGCATATGAGTGCACGAAGTGAGTCA-′), and reverse CR2 (5′-CACTCTCGAGTGGCTGCCCATCTCCTGCTTC-3prime]); and forward LU1 (5′-TGCATGTGTGTTGTCCTTCAG-3′), and reverse LU2 (5′-GAGTTCCCAGTGCTATGTGCTGCT-3′). All of the primers were synthesized by Genosys (The Woodlands, TX).

Constructs. The pCI-*PAGE4* plasmid was constructed from the pLZR-SpBMN-Z vector (3) replacing the *lacZ* gene with the *PAGE4* cDNA. The DNA fragment encoding the open reading frame of *PAGE4* was amplified from the *PAGE4* cDNA using primer pairs CP1 and CP2. The PCR product was gel purified, digested with *Eco*RI, and ligated into an *Eco*RI-digested pLZR-SpBMN-Z vector. The pET-*PAGE4* plasmid was constructed using the pET23a plasmid (Novagen, Madison, WI). The DNA fragment encoding the open reading frame of *PAGE4* was amplified from the *PAGE4* cDNA using primer pairs CR1 and CR2. The PCR product was gel purified, digested with *Nde*I and *Xho*I, and ligated into a *Nde*I-*Xho*I-digested pET23a vector.

The pBS-*PAGE4* plasmid was constructed using the pBluescript II SK (+) plasmid (Stratagene, La Jolla, CA). The pBS-*PAGE4* plasmid contains the nucleotides 1–442 of the *PAGE4* transcript.

Received 11/23/01; revised 1/28/02; accepted 1/28/02.

[1] Present address: Novartis Pharmaceuticals Corporation, 9 West Watkins Mill Road, Gaithersburg, Maryland 20878.

[2] To whom reprint requests should be addressed, at Laboratory of Molecular Biology, Clinical Cancer Research, National Cancer Institute, NIH, 37 Convent Drive MSC 4264, Building 37, Room 5106, Bethesda, MD 20892-4264. Phone: (301) 496-0976; Fax: (301) 402-1344; E-mail: tkbera@helix.nih.gov.

[3] The abbreviations used are: EST, expressed sequence tag; CT, cancer-testis; Dlk1, δ-like homologue *Drosophila*; IGFbp-2, insulin-like growth factor binding protein 2; LPL, lipoprotein lipase; RT-PCR, reverse transcription-PCR; NCI, National Cancer Institute; CCR, Clinical Cancer Research.

Cell Lines and Culture. NIH3T3 and 293T cells were maintained at 37°C in 5% CO_2 in DMEM supplemented with 10% fetal bovine serum (Quality Biological, Inc., Gaithersburg, MD), 2 mM L-glutamine, and 1 mM penicillin-streptomycin. PC3 cells were maintained at 37°C in 5% CO_2 in RPMI medium supplemented with 10% fetal bovine serum (Quality Biological), 2 mM L-glutamine, 1 mM sodium pyruvate and penicillin-streptomycin.

Packaging Cells Transfection and Target Cells Infection. The amphotropic 293T packaging line was transfected by a calcium-phosphate/chloroquine method described previously (3). Culture supernatants containing viral particles were collected 48 h after transfection, filtered with a 0.22 μm filter unit (Millipore, Bedford, MA), and used to infect the target cells. For stable infections, cells were plated in dishes of 100 mm at low density (300 cells/dish) and medium density (1000 cells/dish) 48 h after the infection. Three days after the infection, NIH3T3 cells were selected with 2.5 μg/ml puromycin, and PC3 cells were selected with 0.5 μg/ml puromycin. After 15 days, individual clones were picked and grown in the absence of puromycin.

Comparative cDNA Microarray Analysis. The protocol used for microarray analysis was designed by the Microarray Core Facility at NCI and can be found on the NCI/CCR microarray homepage.[4] Mm-OC-6.1p mouse array chips were obtained from the NCI microarray core facility. After hybridization, arrays were scanned using an Axon GenePix 4000 scanner and processed using the GenePix software. The results were analyzed using tools found on the NCI/CCR microarray homepage.

RNA Isolation for Microarray Analysis. Total RNA was isolated from the clones infected with pCI-*PAGE4*, pLZR-SpBMN-Z, and the empty vector. The RNA was prepared by using TRIzol Reagent according to the manufacturer's instructions (Life Technologies, Inc., Rockville, MD) with the following modifications: after the chloroform addition and the phase separation, the aqueous phase was used in a second round of purification using the Rneasy Maxi Kit (Qiagen, Chatsworth, CA) as recommended by the manufacturer.

mRNA Extraction and Northern Analysis. mRNA from each cell line was isolated using a FastTrack kit (Invitrogen, Carlsbad, CA). Two μg mRNA per lane were electrophoresed under denaturing conditions and subsequently transferred to a nylon membrane according to established procedure. The *PAGE4* cDNA fragment was labeled with ^{32}P by random primer extension (Lofstrand Labs Ltd., Gaithersburg, MD). Hybridization was performed as described previously (4).

Dot Blot Analysis of Matched Tumor/Normal Expression Array. A membrane with 68 separate samples of cDNA synthesized from human tumors and corresponding normal tissue from the same individual (Clontech, Palo Alto, CA) was hybridized with a ^{32}P-labeled *PAGE4* cDNA fragment (Lofstrand Labs Ltd.). Hybridization conditions were described previously (4).

[4] Internet address: http://nciarray.nci.nih.gov/.

RT-PCR. For the analysis of LPL expression on PC3 and prostate mRNA, RT-PCR was performed as described previously (4) using primer pair LU1 and LU2.

***In Situ* Hybridization.** The paraffin-embedded prostate tissue sections were deparaffinized by placing the slides over a slide warmer at 65°C for 1 h. The slides were then rinsed in two changes of xylene for 5 min each and air-dried. They were then rinsed in two changes of absolute alcohol for 5 min and air-dried. Biotinylated probes were prepared using *PAGE4* (442 bp) and U6 (250 bp) cDNA cloned in pBluescript II (+) plasmid. Biotinylated pBluescript II (+) without any insert was used as negative control. Probes were labeled using the BioNick Labeling System kit (Life Technologies, Inc., Rockville, MD) according to the manufacturer' s instructions. The probes were incubated at 16°C for 3 h. The unincorporated nucleotides from the labeled DNA probe were removed by three ethanol precipitations. Slides were hybridized using the *In Situ* Hybridization and Detection system (Life Technologies, Inc.) according to the manufacturer' s instructions. The slides were counterstained using 0.2% Light Green stain, rinsed through a series of alcohol grades, and mounted in Cytoseal. Microscopic evaluation (brightfield) was performed using a Nikon Eclipse 800 microscope (5).

Preparation of Cell Extracts. Protein extracts from different cell lines were prepared as described previously (6). Briefly, about 5×10^6 growing cells (80% confluent) from each respective cell line were harvested and resuspended in 1× RIPA buffer containing proteinase inhibitors [50 mM Tris-HCl (pH 7.5), 150 mM NaCl, 1 mM EDTA, 0.1% Triton X-100, 1 mM phenylmethylsulfonyl fluoride, 10 μg/ml aprotinin, and 10 μg/ml leupeptin]. The extracts were rotated for 30 min at 4°C and clarified by centrifugation. Protein concentrations were determined by using the Coomassie Plus Protein Assay reagent according to the manufacturer's instructions (Pierce, Rockport, IL).

Protein extracts from normal prostate and prostate cancer tissue were prepared by grinding 0.5 g of tissue frozen at −80°C into a fine powder using a cold mortar and pestle. The powdered tissue was collected, resuspended in 1× RIPA buffer, and sonicated briefly and clarified by centrifugation.

Nuclear, membrane, and cytoplasmic extracts from NIH3T3 and PC3 cells, infected with *PAGE4*, were prepared based on published protocols (7, 8).

Preparation of Recombinant PAGE4 Protein. The plasmid pET-*PAGE4* encodes amino acids 1 to 102 of *PAGE4* with six histidines at the COOH terminus encoded by the vector to facilitate purification of the protein. The recombinant PAGE4 protein was then expressed in *Escherichia coli* and purified using Ni^{2+}NTA agarose matrix following the supplier's instructions (Qiagen Inc.).

Production of Polyclonal Anti-PAGE4 Antibodies in Rabbits and Purification of IgG from Antisera. Purified PAGE4 protein was diluted to 0.5 mg/ml and injected into rabbits with complete Freund's adjuvant for the first immunization, and with incomplete Freund's adjuvant for subsequent immunizations. For PAGE4 antipeptide antibody, a peptide of 15 amino acids (amino acids 46–63) was synthesized and then injected into rabbits as described above. Sera

were collected after the fourth, fifth, and sixth immunizations and titrated by ELISA against the purified recombinant PAGE4 protein. Total IgG was then purified with immobilized protein A (Pierce) matrix following the supplier's instructions.

For tissue analysis, the *PAGE4* antisera were further purified by using immobilized *E. coli* lysate kit (Pierce) according to the manufacturer's instructions. The *PAGE4*-peptide antisera were further affinity-purified by using a HiTrap *N*-hydroxy-succinimide-activated column coupled with the recombinant *PAGE4*, according to the manufacturer's instructions.

Western Blot Analysis. Ten μg of protein extract from cell lines and 80 μg from tissues were run on a 16.5% Tris-Tricine gel (BIO-RAD, Hercules, CA) and transferred to a 0.2 μm Immun-Blot polyvinylidine difluoride membrane (BIO-RAD) in transfer buffer [25 mM Tris, 192 mM glycine, 20% (v/v) methanol (pH 8.3)] at 4°C for 2 h at 50 V. Filters were probed with 10 μg/ml protein A-purified anti-*PAGE4* antiserum or 1 μg/ml affinity column-purified anti-*PAGE4*-peptide antiserum, and their respective signals were detected using a chemiluminescence Western blotting kit according to the manufacturer's instructions (Roche Molecular Biochemicals, Indianapolis, IN).

Immunofluorescence Analysis. Immunofluorescence analysis was performed as previously described (9). Briefly, 293T and NIH3T3 cells, transfected with pCI-*PAGE4* plasmid, were grown in 35-mm dishes. Cells were then fixed in 3.7% formaldehyde in PBS for 15 min at 23°C and then washed in PBS. All of the subsequent incubations (at 23°C) included 0.1% saponin (Sigma Chemical Co., St. Louis, MO) and 1% BSA in PBS (BSA-sap-PBS). Fixed cells were first incubated in BSA-sap-PBS for 30 min and then incubated with affinity-purified anti-PAGE4 antibodies (10 μg/ml) for 30 min. After washing in PBS, the cells were incubated with affinity-purified goat antirabbit IgG (H+L) conjugated to rhodamine (25 μg/ml) in BSA-PBS for 30 min. After washing, cells were fixed in 3.7% formaldehyde and mounted under coverslips in buffered glycerol. Microscopic evaluation of cells expressing PAGE4 protein was performed by direct observation of cells using a Zeiss Axiplan2 fluorescent microscope equipped with rhodamine filters, and images were captured using a Dage 300 cooled-chip charge coupled device camera.

Results

Expression of *PAGE4* in Various Cancers. By using Northern blot and RT-PCR analysis, we previously reported that *PAGE4* is expressed in normal prostate, prostate cancer, and female reproductive tissues (2). To determine whether *PAGE4* is expressed in other types of cancer, we conducted a cDNA dot blot analysis using a cancer-profiling array (Clontech). This array contains samples from 68 different cancers and their corresponding normal tissues. As shown in Fig. 1, among the 68 different samples from human normal and cancer tissues, *PAGE4* was detected in all three of the normal prostate samples (D11, 12, and 13) and prostate cancer samples (E11, 12, and 13). Moreover, *PAGE4* was found in one normal cervix sample and cervical cancer sample (G14 and H14, respectively). *PAGE4* was also detected in four uterine cancer samples (H1, 3, 4, and 5), three normal uterus samples (G3, 4, and 5), and one ovary sample (G10). Interestingly, the expression of *PAGE4* was also found in two kidney cancer samples (B2 and 5) but not in normal kidney (A1–A11).

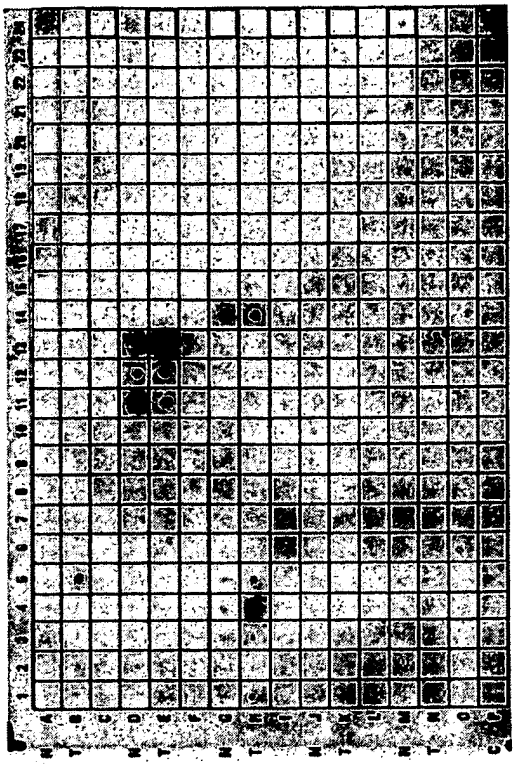

Fig. 1. Dot blot analysis of *PAGE4* probe. Hybridization of *PAGE4* probe on a matched tumor (*T*)/normal (*N*) expression array membrane (Clontech) showed specific hybridization of *PAGE4* in different samples. Samples on the blot are from kidney (*A* and *B*, *1–11*), breast (*D* and *E*, *1–9*), prostate (*D* and *E*, *11–13*), uterus (*G* and *H*, *1–7*), ovary (*G* and *H*, *9–12*), cervix (*G* and *H*, *14*), colon (*J* and *K*, *1–11*), lung (*J* and *K*, *13–15*), stomach (*M* and *N*, *1–8*), rectum (*M* and *N*, *10–16*), and small intestine (*M* and *N*, *19*).

***PAGE4* mRNA Is Expressed in Epithelial Cells of Normal Prostate and Prostate Cancer.** The RNA used for both dot blot and RT-PCR analyses was extracted from whole tissue, which consisted of mixed populations of epithelial cells, smooth muscle cells, and fibroblasts, as well as other cell types. To determine the cell types that express the *PAGE4* mRNA in normal prostate as well as in prostate cancer tissue, we used *in situ* hybridization with biotin-labeled *PAGE4* cDNA as described in "Materials and Methods." As shown in Fig. 2, *PAGE4* mRNA was highly expressed in prostatic epithelial cells of normal prostate (*A*) and in prostate cancer tissue (*B*). There was no detectable signal in cells of the stromal compartment, which suggests that *PAGE4* was specifically expressed in the epithelial cells of the prostate.

***PAGE4* mRNA Encodes for a M_r 16,000 Cytoplasmic Protein.** We reported previously that the *PAGE4* transcript has a predicted open reading frame of 102 amino acids,

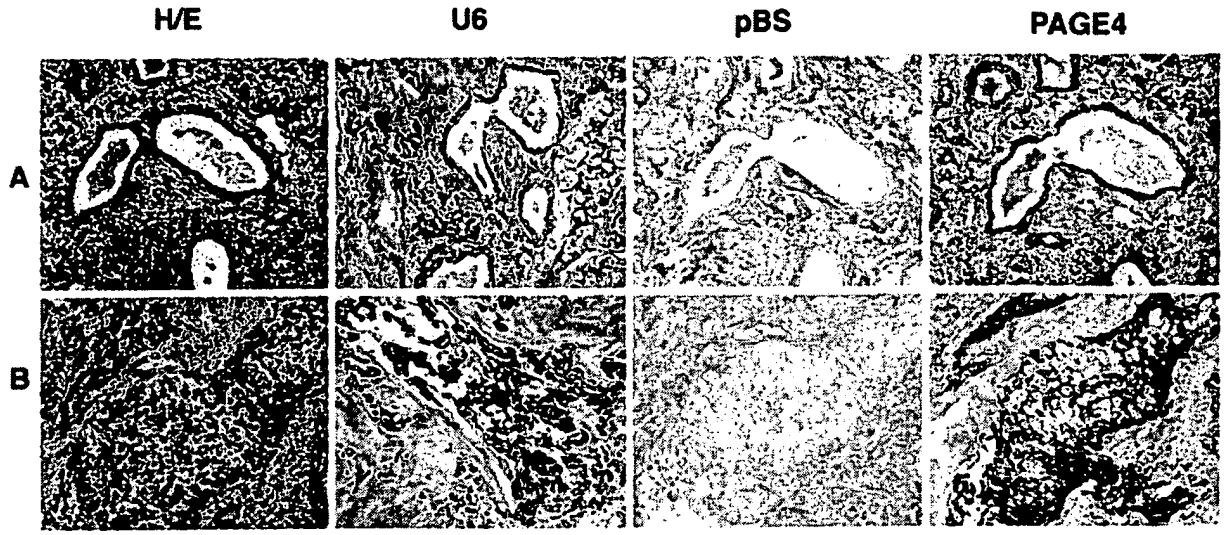

Fig. 2. In situ localization of *PAGE4* mRNA expression. *In situ* hybridization of normal prostate and prostate cancer tissue. *A*, H&E (*H/E*) stains of a representative field of benign prostatic ducts. *PAGE4* is strongly expressed in atrophic basaloid type epithelium. *B*, an example of solid lobular adenocarcinoma, Gleason grade 4 (score 8/10) strongly expressing *PAGE4*. The *PAGE4* signal is comparable in intensity with U6 positive control, in contrast to pBS negative control.

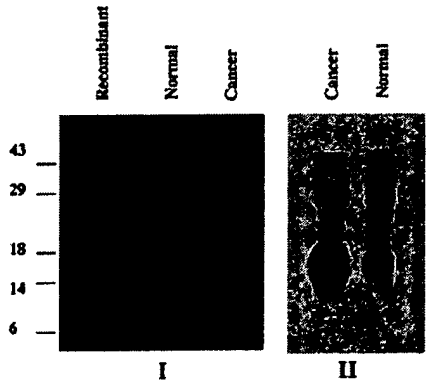

Fig. 3. Western blot analysis of PAGE4 protein. PAGE4 protein is detected in normal prostate and prostate cancer lysate. Protein extracts from normal prostate and prostate cancer (80 μg each) were analyzed on a Tris-tricine 16.5% PAGE and blotted with either antipeptide (*I*) or anti-full-length PAGE4 (*II*) polyclonal antibodies. Purified recombinant PAGE4 (10 ng) protein was used as a positive control.

which can generate a protein of M_r 11,900 in size. To determine the size of PAGE4 protein expressed in normal prostate and in prostate cancer tissue, we generated polyclonal rabbit antibodies against a chemically synthesized PAGE4 peptide as well as a recombinant PAGE4 protein as described in the "Materials and Methods" section. As shown in Fig. 3, a specific band at a M_r of ~16,000 was detected in protein extracts from normal prostate and prostate cancer by both antibodies. The M_r 16,000 kDa band comigrated with the recombinant PAGE4 protein, which indicated that the band detected in normal prostate and in prostate cancer was PAGE4. We did not detect this band using IgG prepared from preimmune rabbit serum or using a brain tissue extract but we did find expression of PAGE4 in placenta which is known to express *PAGE4* mRNA (data not shown).

To determine the location of PAGE4 protein in the cell, we performed two sets of experiments. In the first experiment, we prepared nuclear, cytoplasmic, and membrane fractions from NIH3T3 and PC3 cells stably expressing *PAGE4*. As shown in Fig. 4*A*, a specific M_r 16,000 PAGE4 product, which comigrates with recombinant PAGE4, was detected only in the cytoplasmic fraction of both of the cell lines, and not in the nuclear or membrane fractions. In a second experiment, we transfected 293T cells and infected NIH3T3 cells transiently with an expression (pCI-*PAGE4*) plasmid and performed an immunofluorescence experiment with anti-PAGE4 antibody. As shown in Fig. 4*B*, an intense cytoplasmic staining was observed in both NIH3T3 and 293T cells, which were transfected with *PAGE4* cDNA, indicating that PAGE4 protein is localized in the cytoplasm of the cells. No staining was observed in cells transfected with empty vector (data not shown).

PAGE4-regulated Gene Expression in Infected NIH3T3 and PC3 Cell Lines. Although many CT antigens have now been reported, very little is known about their biological functions. We investigated the ability of *PAGE4* to alter gene expression in the mouse NIH3T3 cell line. NIH3T3 cells do not express *PAGE4* mRNA. We generated several stable cell lines expressing the *PAGE4* transcript and protein; for the analysis, we pooled the RNA from three different stable of lines NIH3T3. To identify the transcript, which could be differentially regulated in the presence or absence of *PAGE4*, we used cDNA microarray hybridization, because it allowed us to screen numerous transcripts simultaneously. The mouse array used in this study contains 2688 cDNAs including known genes and ESTs from unknown genes (Mm-OC-6.1p).[4] Genes that were either up- or down-regulated at least

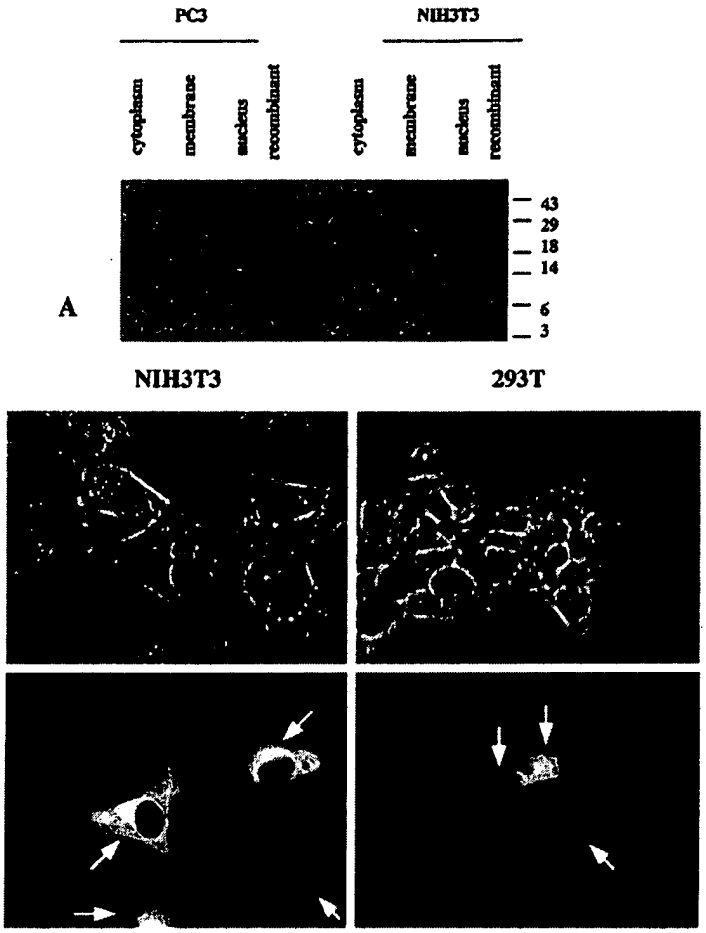

Fig. 4. Detection of PAGE4 protein on transfected cells. *A*, PAGE4 protein is detected in the cytoplasmic fraction of the cell. Protein extracts (cytoplasm, membrane, and nuclear fraction) from *PAGE4*-transfected NIH3T3 and PC3 cell lines were analyzed on a Tris-tricine 16.5% PAGE. Ten μg of protein extract was loaded on each lane. For positive control, 10 ng of recombinant *PAGE4* was loaded. *B*, *PAGE4*-transfected NIH3T3 and 293T cells were fixed, permeabilized using saponin, and incubated with anti-PAGE4 antibodies, followed by an antirabbit IgG-rhodamine conjugate. Intense cytoplasmic staining (*arrows*) was observed in both cell lines.

Table 1 Genes up/down-regulated in PAGE4 and β galactosidase (β Gal) stable cell lines

Gene	NIH3T3		PC3	
	PAGE4	β Gal	PAGE4	β Gal
Dlk1	↑[a]	↑	noc	noc
IGFBP 2	↑	↑	–	–
LpL	↓	–	–	–
SCGN-10[b]	noc	noc	↓	↓

[a] ↑, up-regulated; ↓, down-regulated; –, no change; noc, not on chip.
[b] SCGN-10, uperior cervical ganglia, neural-special 10.

2.5-fold in *PAGE4*-transfected cells, but not in β-galactosidase-transfected cells, were considered for analysis.

Only three genes were found to be altered by 2.5-fold or more (Table 1). One of the genes, that was specifically modulated in *PAGE4*-transfected cells as compared with vector-alone-transfected cells, was *LPL*. LPL is the primary enzyme responsible for the conversion of lipoprotein triglycerides into free fatty acids and monoglycerides. *LPL* was reproducibly down-regulated in *PAGE4*-expressing stable cells (Fig. 5*A*), as compared with vector-alone-transfected or β-galactosidase-transfected cell lines. Two other genes, *Dlk1* and *IGFbp-2*, were up-regulated in *PAGE4*-transfected cells, but they were also up-regulated in β-galactosidase-transfected NIH3T3 cells (Table 1). Thus, this effect of *PAGE4* was not specific. Down-regulation of *LPL* expression in *PAGE4* stable lines was verified by Northern blot analysis. RNA was isolated from each of three independent cell lines that were transfected with either *PAGE4* or empty vector, and that were subjected to Northern analysis using a radiolabeled *LPL* cDNA probe. As shown in Fig. 5*B*, all three of the cell lines stably expressing *PAGE4* had undetectable *LPL* mRNA expression as compared with the cells infected with empty vector or vector expressing the *β-galactosidase* gene.

We then investigated the ability of *PAGE4* to alter gene expression in the PC3 prostate cancer cell line. PC3 is an androgen-independent prostate-cancer cell line and does not express *PAGE4* mRNA.[5] We generated several stable cell lines expressing the PAGE4 transcript and protein, and we analyzed RNA expression with an array that contains 6538 human cDNAs including known genes and ESTs from unknown genes.[4] We found that none of the cDNAs was significantly modulated in the PC3 cells expressing *PAGE4*

[5] Iavarone and Bera, unpublished observations.

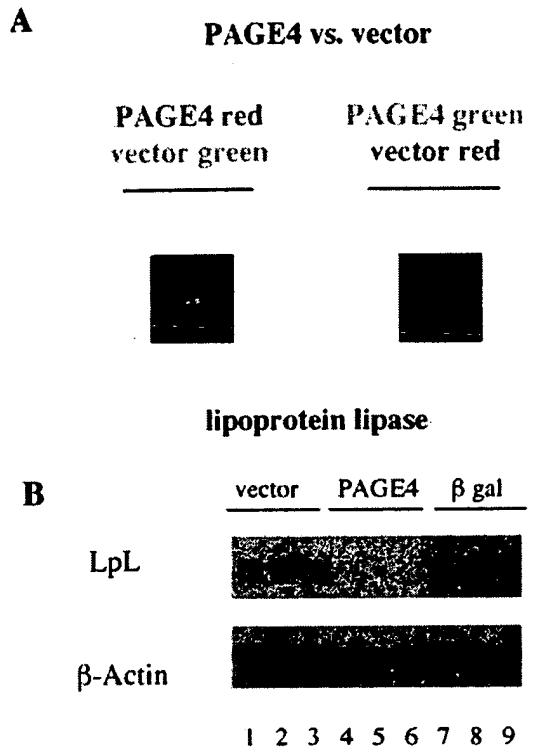

Fig. 5. *PAGE4*-mediated differential gene expression in transfected NIH3T3 cells. *A*, gene expression profiling of *PAGE4*-transfected and vector-alone-transfected NIH3T3 cells by microarray analysis. The same spot (*LPL*) is detected by two independent experiments in which *PAGE4*-transfected cell RNA is labeled with red or green dye. In *B*, LPL transcript is down-regulated in *PAGE4*-transfected 3T3 cells. An equal amount (2 μg) of polyadenylate RNA from NIH3T3 cells (three independent clones), transfected with either *PAGE4* or vector alone, was size-fractionated and transferred to nitrocellulose filter. Filters were then hybridized with labeled LPL cDNA as described in "Materials and Methods." The filters were stripped and reprobed with labeled actin to determine equal loading of RNA in the membrane.

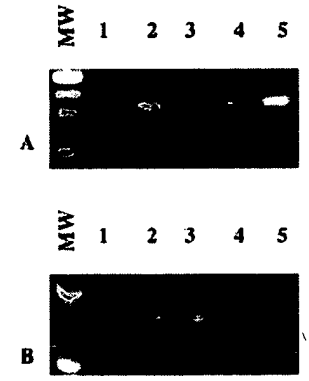

Fig. 6. RT-PCR and PCR analyses of *LPL* gene in PC3 cell line. Ethidium bromide-stained 1.2% agarose gels: in *A*, *LPL* cDNA was amplified with specific primers for the 3′ untranslated region of *LPL* mRNA. A specific band was amplified by using normal prostate cDNA (Clontech; *Lane 2*), PC3 genomic DNA (*Lane 4*) and human genomic DNA (*Lane 5*). No band was amplified without template (*Lane 1*) and using PC3 cDNA (*Lane 3*). In *B*, integrity of each mRNA and genomic DNA samples used was tested by amplifying the *actin* gene using specific primers for actin.

including LPL, which was down-regulated in mouse array analysis (see below).

Discussion

PAGE4 is a CT antigen expressed in normal prostate, testis, and placenta, and highly expressed in prostate and uterine cancer. In this report, we demonstrate that *PAGE4* mRNA expression is restricted to the epithelial cells of normal prostate and prostate carcinomas. The PAGE4 protein is M_r 16,000 in size and is localized in the cytoplasmic compartment of the cell. To investigate the function of *PAGE4*, we introduced *PAGE4* into a mouse fibroblast cell line (NIH3T3) and also into a prostate cancer cell line (PC3) and found that LPL is down-regulated in NIH3T3 cells expressing *PAGE4*, but not in PC3 cells.

Expression of PAGE4 Affects *LPL* Gene Expression. LPL, a rate-limiting enzyme responsible for the hydrolysis of circulating triglyceride, is bound to the luminal surface of capillary endothelium in adipose tissue and muscle (10). Although LPL is functional at the surface of the endothelial cells, it is not clear which cells synthesize the enzyme and what the cellular distribution of LPL is within the tissue. It has been reported that the expression of the *LPL* gene is regulated by progesterone and protein kinase A in undifferentiated hepatoma cells (11). Reduction in LPL activity has been implicated in cachexia in cancer patients. Cachexia is a common feature of malignant disease and is characterized by marked weight loss, anorexia, and extensive breakdown of body fat and skeletal protein because of homeostatic disturbances (12). It has been reported that the *LPL* gene in humans is localized on chromosome 8p22 (13), and there is a frequent allelic loss of chromosome 8p22 loci in human prostate cancer. Because we observed down-regulation of LPL in NIH3T3 cells expressing *PAGE4*, but not in the prostate cancer cell line PC3, we investigated whether the *LPL* gene is expressed in the PC3 cell line. As shown in Fig. 6*A*, *Lane 3*, the *LPL* gene is not expressed in the PC3 cell line, thus, *PAGE4* could not possibly down-regulate LPL expression in this cell line. To determine whether the *LPL* gene is deleted in PC3 cells, we did a PCR analysis on chromosomal DNA isolated from PC3 cells. As shown in Fig. 6*A*, *Lane 4*, the intensity of the PCR product from PC3 DNA is one-half the intensity of the PCR product (Fig. 6*A*, *Lane 5*) obtained from normal human chromosomal DNA, which suggests that at least one of the *LPL* alleles is deleted in PC3 cells. Further analysis of the PC3 cell line is needed to establish the exact copy number of the *LPL* gene in PC3 cells, and the significance of the LPL deletion in prostate cancer and its down-regulation by *PAGE4* gene needs further study.

Although CT antigens have been identified for over a decade, no function has been described for these antigens in the literature. These antigens are encoded quite frequently by genes located on the X chromosome. There is speculation that some CT gene products are transcriptional factors, but there is no direct experimental evidence supporting that concept. Two of the previously reported CT antigens, SCP-1 and CT9 have small basic domains and several conserved motifs, which are characteristics of DNA-binding proteins

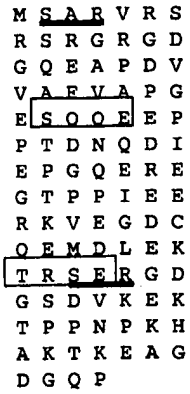

Fig. 7. Amino acid analysis of PAGE4. Amino acid sequence analysis of PAGE4 was performed using the PROSITE program. *Underlined*, two potential protein kinase C phosphorylation sites (amino acids 2–4 and 73–75) contained in PAGE4 protein. *Boxed*, two potential casein kinase 2 phosphorylation sites (amino acids 30–33 and 71–74).

(14, 15). Amino acid sequence analysis of *PAGE4* showed no such motifs in the PAGE4 protein.

At this point, it is not clear whether the regulatory effect of *PAGE4* on the *LPL* gene is direct or indirect. Because PAGE4 protein is localized in the cytoplasm of the cell, it is more likely that *PAGE4* indirectly regulates the expression of the *LPL* gene. It is also possible that *PAGE4* is posttranslationally modified and involved in a signal transduction pathway. Analysis of the *PAGE4* amino acid sequence using the PROSITE program of the Swiss Institute of Bioinformatics ExPASy proteomics server[6] (16, 17) predicts several potential phosphorylation sites. As shown in Fig. 7 there are two casein kinase 2 (SQQE and TRSE) sites and two protein kinase C phosphorylation sites (SAR and SER). The significance of these phosphorylation sites, as well as the mechanism by which *PAGE4* alters the expression of the *LPL* gene, is yet to be determined. To our knowledge, this is the first report of CT antigen-mediated gene regulation in the literature.

PAGE4, a CT Antigen, Is a Potential Target for Cancer Vaccines. CT antigens are a distinct class of antigens that have a restricted pattern of expression in essential tissue and aberrant expression in many different tumor types (18). CT antigens are often expressed at higher levels in testis and placenta, which are known to express only low amounts of MHC class I molecules. Thus, expression of CT antigens in these normal tissues should not lead to T-cell activation and this makes these antigens attractive candidates for cancer vaccines (19). Our earlier studies demonstrated that *PAGE4* is expressed in prostate and uterine cancer. Data presented here indicate that *PAGE4* is also expressed in cervical, ovarian, and kidney cancer and increases its attractiveness as a cancer vaccine target.

Acknowledgments

We thank Verity Fogg for cell culture and Anna Mazzuca for editorial assistance.

[6] Internet address: http://www.expasy.ch.

References

1. Vasmatzis, G., Essand, M., Brinkmann, U., Lee, B., and Pastan, I. Discovery of three genes specifically expressed in human prostate by expressed sequence tag database analysis. Proc. Natl. Acad. Sci. USA, *95:* 300–304, 1998.

2. Brinkmann, U., Vasmatzis, G., Lee, B., Yerushalmi, N., Essand, M., and Pastan, I. *PAGE-1*, an X chromosome-linked GAGE-like gene that is expressed in normal and neoplastic prostate, testis, and uterus. Proc. Natl. Acad. Sci. USA, *95:* 10757–10762, 1998.

3. Kinisella, T. M., and Nolan, G. P. Episomal vectors rapidly and stably produce high-titer recombinant retrovirus. Hum. Gene Ther., *7:* 1405–1413, 1996.

4. Liu, X. F., Olsson, P., Wolfgang, C. D., Bera, T. K., Duray, P., Lee, B., and Pastan, I. PRAC: a novel small nuclear protein that is specifically expressed in human prostate and colon. Prostate, *47:* 125–131, 2001.

5. Kumar, V., and Collins, F. H. A technique for nucleic acid *in situ* hybridization to polytene chromosomes of mosquitoes in the *Anopheles gambiae* complex. Insect Mol. Biol., *3:* 41–47, 1994.

6. Wolfgang, C. D., Essand, M., Vincent, J. J., Lee, B., and Pastan, I. TARP: a nuclear protein expressed in prostate and breast cancer cells derived from an alternate reading frame of the T cell receptor γ chain locus. Proc. Natl. Acad. Sci. USA, *97:* 9437–9442, 2000.

7. Dignam, J. D., Lebovitz, R. M., and Roeder, R. G. Accurate transcription initiation by RNA polymerase II in a soluble extract from isolated mammalian nuclei. Nucleic Acids Res., *11:* 1475–1489, 1983.

8. Sladek, F., M., Zhong, W. M., Lai, E., and Darnell, J. E., Jr. Liver-enriched transcription factor HNF-4 is a novel member of the steroid hormone receptor superfamily. Genes Dev., *4:* 2353–2365, 1990.

9. Chang, K., Pastan, I., and Willingham, M. C. Isolation and characterization of a monoclonal antibody, K1, reactive with ovarian cancers and normal mesothelium. Int. J. Cancer, *50:* 373–381, 1992.

10. Goldberg, I. J., and Merkel, M. Lipoprotein lipase: physiology, biochemistry, and molecular biology. Front. Biosci., *6:* 388–405, 2001.

11. Peinadoonsurbe, J., Staels, B., Deeb, S., and Auwerx, J. Lipoprotein-lipase expression in undifferentiated hepatoma-cells is regulated by progesterone and protein kinase-A. Biochemistry, *31:* 10121–10128, 1992.

12. DeWys, W. D., Begg, C., Lavin, P. T., Band, P. R., Bennett, J. M., Bertino, J. R., Cohen, M. H., Douglass, H. O., Engstrom, P. F., Ezdinli, E. Z., Horton, J., Johnson, G. J., Moertel, C. G., Oken, M. M., Perlia, C., Rosenbaum, C., Silverstein, M. N., Skeel, R. T., Sponzo, R. W., and Tormey, D. C. Prognostic effect of weight-loss prior to chemotherapy in cancer-patients. Am. J. Med., *69:* 491–497, 1980.

13. Bova, G. S., Carter, B. S., Bussemakers, M. J., Emi, M., Fujiwara, Y., Kyprianou, N., Jacobs, S. C., Robinson, J. C., Epstein, J. I., Walsh, P. C., and Isaacs, W. B. Homozygous deletion and frequent allelic loss of chromosome 8p22 loci in human prostate cancer. Cancer Res., *53:* 3869–3873, 1993.

14. Jones, M. H., Numata, M., and Shimane, M. Identification and characterization of *BRDT*: a testis-specific gene related to the bromodomain genes *RING3* and *Drosophila fsh*. Genomics, *45:* 529–534, 1997.

15. Meuwissen, R. L. J., Offenberg, H. H., Dietrich, A. J. J., Riesewijk, A., Vaniersel, M., and Heyting, C. A coiled-coil related protein-specific for synapsed regions of meiotic prophase chromosomes. EMBO J., *11:* 5091–5100, 1992.

16. Appel, R. D., Bairoch, A., and Hochstrasser, D. F. A new generation of information retrieval tools for biologists: the example of the ExPASy WWW server. Trends Biochem. Sci., *19:* 258–260, 1994.

17. Hofmann, K., Bucher, P., Falquet, L., and Bairoch, A. The PROSITE database, its status in 1999. Nucleic Acids Res., *27:* 215–219, 1999.

18. Ono, T., Kurashige, T., Harada, N., Noguchi, Y., Saika, T., Niikawa, N., Aoe, M., Nakamura, S., Higashi, T., Hiraki, A., Wada, H., Kumon, H., Old, L. J., and Nakayama, E. Identification of proacrosin binding protein sp32 precursor as a human cancer/testis antigen. Proc. Natl. Acad. Sci. USA, *98:* 3282–3287, 2001.

19. Moingeon, P. Cancer vaccines. Vaccine, *19:* 1305–1326, 2001.

This Page is Inserted by IFW Indexing and Scanning Operations and is not part of the Official Record

BEST AVAILABLE IMAGES

Defective images within this document are accurate representations of the original documents submitted by the applicant.

Defects in the images include but are not limited to the items checked:

- ☐ BLACK BORDERS
- ☐ IMAGE CUT OFF AT TOP, BOTTOM OR SIDES
- ☐ FADED TEXT OR DRAWING
- ☑ BLURRED OR ILLEGIBLE TEXT OR DRAWING
- ☐ SKEWED/SLANTED IMAGES
- ☐ COLOR OR BLACK AND WHITE PHOTOGRAPHS
- ☐ GRAY SCALE DOCUMENTS
- ☐ LINES OR MARKS ON ORIGINAL DOCUMENT
- ☐ REFERENCE(S) OR EXHIBIT(S) SUBMITTED ARE POOR QUALITY
- ☐ OTHER: _____

IMAGES ARE BEST AVAILABLE COPY.
As rescanning these documents will not correct the image problems checked, please do not report these problems to the IFW Image Problem Mailbox.